LEGIBILITY NOTICE

A major purpose of the Technical Information Center is to provide the broadest dissemination possible of information contained in DOE's Research and Development Reports to business, industry, the academic community, and federal, state and local governments.

Although a small portion of this report is not reproducible, it is being made available to expedite the availability of information on the research discussed herein.

LA-UR -90-1820

CONF-

Los Alamos National Laboratory is operated by the University of California for the United States Department of Energy under contract W-7405-ENG-36

LA-UR--90-1820

DE90 012052

TITLE ADVANCES IN SPHEROMAK UNDERSTANDING AND PARAMETERS

AUTHOR(S) J. C. Fernandez, CTR-1

SUBMITTED TO IV Latin American Workshop on Plasma Physics
Buenos Aires, Argentina
July 16-27, 1990

DISCLAIMER

Los Alamos National Laboratory
Los Alamos, New Mexico 87545

Draft May 24, 1990

Review of Advances in Spheromak Understanding and Parameters *

J. C. Fernández

Los Alamos National Laboratory, Los Alamos, NM 87545

A spheromak is a toroidally-shaped magnetized plasma configuration in which no material (such as coils or vacuum vessels) links the torus, so that the topology of the spheromak boundary is spherical. The magnetic fields in the plasma are generated by the internal plasma currents. In the period of ten years since the properties of a nearly force-free ($\nabla \times \vec{B} \approx \lambda \vec{B}$) spheromak configuration were described using single-fluid MHD theory,[M. N. Rosenbluth, M. N. Bussac, Nucl. Fusion **19**, 489 (1979)] remarkable theoretical and experimental advances have been made. This paper highlights some of that work. Spheromaks not only have been successfully produced in the laboratory using a variety of methods, but also translated, compressed and stably sustained for many resistive-decay times. Spheromak formation, equilibrium and stability to current-driven modes have been successfully modeled by single-fluid MHD coupled with the concepts of magnetic helicity (flux linkage) and relaxation towards the minimum-energy force-free state. [J. B. Taylor, Rev. Mod. Phys. **58**, 741 (1986)] There is evidence, however, that the relaxation mechanism which drives parallel plasma currents (to drive the spheromak towards the minimum-energy state) is due to effects beyond the scope of single-fluid resistive MHD. The confinement properties of clean spheromaks (sometimes exceeding 1 MA toroidal current and 1 T volume-average magnetic field) have been measured, and shown to be excellent, provided the fraction of open magnetic flux at the edge is decreased sufficiently. It has been shown theoretically how plasma $\langle \beta \rangle_{vol}$ limits (from the Mercier criterion) of $\approx 10\%$ can be obtained by properly shaping either the conducting wall geometry or the spheromak current profile. (Because of the low fields needed from external coils in steady-state operation in a spheromak fusion reactor, spheromak $\langle \beta \rangle_{vol} \approx 5\%$ is equivalent to 20% in a tokamak.) While plasma β in spheromaks often exceeds the limit from the Mercier criterion, a pressure-driven interchange mode has been directly observed.

Spheromak research is today a truly international endeavor, carried out by groups in Japan, the United Kingdom, Turkey and the United States. In addition to studies directly relating to fusion, the use of spheromaks for other goals is briefly described, including tokamak refueling, radiation production, magnetically-insulated inertially confined fusion, demonstration of helicity injection by mechanical means, and energy storage/transfer to accelerate fast metallic projectiles.

*This work is supported by the US Department of Energy.

Contents

I. Theoretical Background

A. Magnetic equilibria in closed systems

Force-free states ($\vec{J} \parallel \vec{B}$) satisfy the relation

$$\nabla \times \vec{B} = \lambda(\psi)\vec{B}, \tag{1}$$

where $\vec{J}$ and $\vec{B}$ are the current per unit area and magnetic field, and

$$\lambda(\psi) = \mu_0 \vec{J} \cdot \vec{B}/B^2 \tag{2}$$

is constant on magnetic flux surfaces (parametrized by a normalized flux function ψ). In nearly force-free magnetohydrodynamic (MHD) equilibria, such as spheromaks and reversed-field pinches (RFP), it is useful to consider magnetic helicity, which is the linkage of magnetic flux within a closed boundary.[1] For times much shorter than the resistive diffusion time, magnetic helicity conservation has been verified in spheromaks[2-4] and RFPs.[5] When the boundary of the system is a magnetic flux surface (for example, a volume bounded by a perfect conductor with no initial magnetic flux going through the wall), the helicity of the magnetic equilibrium is given by the integral

$$K = \int \vec{A} \cdot \vec{B}\, dvol, \tag{3}$$

where $\vec{A}$ is the vector potential. It should be noted that helicity is a global quantity. Helicity density is not a well defined concept. When the system boundary is not a magnetic surface, Eq.(3) is not gauge invariant. Berger and Field[6] view the problem as arising from the indeterminacy of the flux linkage outside the volume of interest. Their solution is to compare the actual $\vec{B}$ with a reference field $\vec{P}$, such that $\nabla \times \vec{P} = 0$, $\vec{B} \cdot \hat{n} = \vec{P} \cdot \hat{n}$, and $d(\vec{B} \cdot \hat{n})/dt = d(\vec{P} \cdot \hat{n})/dt$. ($\hat{n}$ is the unit vector normal to the surface.) By subtracting the contribution from the reference field, a generalized definition of magnetic helicity,[6] which reduces to Eq.(3) when the system boundary is a magnetic surface, solves the gauge problem. In a system described by Eq.(1) where λ is constant in space,

$$2\mu_0 W/K = \lambda \tag{4}$$

where $W = \int B^2/2\mu_0\, dvol$ is the magnetic energy content of the equilibrium. Of the possible Woltjer-Taylor states[7-11] (constant λ states), one particular state will have minimum magnetic energy per unit helicity at a value $\lambda = \lambda_{me}$ dependent on the system geometry. (In an equilibrium with non spatially constant λ (Sec.III), $2\mu_0 W/K = \langle\lambda\rangle$, where the weighted eigenvalue $\langle\lambda\rangle$ is in practice very close to λ_{me}.) λ can also be considered as the inverse of the characteristic size of the system. In a geometry consisting of coupled subvolumes of different shapes, by expanding into the region of largest characteristic size, the equilibrium can minimize its magnetic energy per unit helicity.[12]

Eq.(1) can be solved analytically in cylindrical geometry, where L is the cylinder length and a is the radius. With the boundary conditions that the radial magnetic field vanishes at the cylinder walls and that there is no net flux, and assuming a spatially constant λ, $\vec{B}$ in Eq.(1) has solutions[13] involving the functions $J_m(\nu_k r)e^{i(m\theta - kz)}$ and $J_{m-1}(\nu_k r)e^{i(m\theta - kz)}$, where r, θ and z are the cylinder's radial, azimuthal and axial coordinates, J_m are the Bessel functions of the first kind, and $\nu_k^2 = \lambda^2 - k^2$ is adjusted to fit

the boundary conditions. For fixed λ, assuming λ and k are purely real, the solutions are a discrete set in m and k. The minimum energy value of λ is determined by the conducting boundary's dimensions. Finn *et al.*[14] showed that in a conducting cylinder of radius a closed on both ends, the $m = 0$ state is the minimum energy state if the cylinder length is less than $1.67a$, whereas the $m = 1$ state is the minimum energy state for longer cylinders. For an infinite cylinder, the $m = 1$ minimum energy state has $\lambda_{me,1}a = 3.112$, while the $m = 0$ minimum energy state has $\lambda_{me,0}a = 3.832$.

Experimentally, the first spheromak ($m = 0$ state) was formed in the PS-1 device at the University of Maryland.[15] The $m = 1$ state (a double helix along L) was first observed at Los Alamos, in what was later named the CTX device, in a copper cylinder with $a = 0.32$ m and $L = 1.2$ m.[16] The pitch of the $m = 1$ double-helix was first measured in a longer $L = 2.1$ m cylinder (unpublished), and subsequently in the $m = 1$ helicity source experiment[12] also at Los Alamos.

Magnetic helicity has handedness. Positive (right-handed) helicity corresponds to $\vec{J}$ parallel to $\vec{B}$, whereas negative (left-handed) helicity corresponds to $\vec{J}$ anti-parallel to $\vec{B}$. There appears to be no intrinsic difference between the two signs of helicity, and stable spheromaks with both signs of helicity have been made.

B. Externally coupled states

A further theoretical refinement (still with spatially constant λ) is to consider externally coupled states,[17,13] in which finite magnetic flux and plasma currents cross the system boundary. For these externally coupled states, the continuum of solutions in λ for each m and k are dependent on the boundary conditions.

In an infinite cylinder, still with λ constant and no radial field at the wall, but with non-zero net axial flux ϕ_z, the locus of solutions to Eq.(1) determine the F-Θ curve,[10] where $F = \pi a^2 B_z(a)/\phi_z$ is the normalized toroidal magnetic field at the wall and $\Theta = \pi a^2 \vec{B}_\vartheta(a)/\phi_z$ is a measure of the axial current. At low current, F is unity, and the fields are tokamak-like. As Θ increases, F monotonically decreases, and the equilibrium corresponds to that of an ultra-low-q tokamak. F crosses zero at $\Theta = 1.2$. At this point, the fields resemble those of a stabilized z-pinch, or equivalently, a straight spheromak. At higher Θ, the toroidal field at the wall reverses, and the fields are RFP-like. Up to $\theta = 1.6$, the minimum energy state has $m = 0$ symmetry. Above 1.6, the axial current is too high for the given axial flux, and the $m = 1$ state has lower energy instead. The result is that the RFP fields develop a helical kink distortion.[8] The RFP literature, starting with the results from the Zeta device at Culham, describes extensive experimental results which confirm the general features of this model.[8,10]

Schaffer[13] considered the case of a complex wavenumber $k = k_r + ik_i$ for externally coupled $m = 0$ and $m = 1$ states in a finite conducting cylinder with open ends and no net axial flux. For the $m = 1$ state with λ between zero and $\lambda_{me,1}$ this model predicts evanescent (complex k) magnetic fields along the length of the tube. For the $m = 0$ state, when λa is below $\lambda_{me,0}$, k is purely imaginary, while for λa above $\lambda_{me,0}a$, k is purely real.

In spite of the good agreement between the spatially constant λ hypothesis with experimental observations, departures from this hypothesis have been routinely observed on CTX spheromaks,[9] the $m = 1$ helicity source experiment,[12] as well as in the ZT-40M RFP.[18] These arise from modifications to the current density profile by spatial nonuniformities of effects such as current drive or electrical resistivity. Therefore, the comparison

of the observed magnetic structures to the theoretical results described above represents a starting point only. On the other hand, experimental observations can be very well modeled numerically by using physically reasonable $\lambda(\psi)$ profiles. But over a wide range of profiles, the qualitative features of the minimum energy states (spheromaks, double-helix, RFP) described above are preserved.

C. Helicity injection

Inside a volume bounded by a magnetic surface, Taylor's hypothesis[8] states that helicity is conserved for times short compared to the resistive decay time, while much faster relaxation processes allow reconnection of magnetic field lines, resulting in a final configuration where the magnetic energy is minimized. The helicity in the system decays resistively at a rate given by[19,6]

$$\frac{dK}{dt} = -2 \int \vec{E} \cdot \vec{B} \, dvol. \tag{5}$$

However, when magnetic fields penetrate the boundary, the helicity can be injected into (or ejected from) the system. The total time derivative of the generalized helicity, derived independently by Jensen and Chu[19] and by Berger and Field,[6] can be conveniently expressed by the relation[20]

$$\frac{dK}{dt} = -2 \int \vec{E} \cdot \vec{B} \, dvol + 2 \int \vec{E}_v \cdot \vec{B}_v \, dvol, \tag{6}$$

or equivalently,

$$\frac{dK}{dt} = -2 \int \oint \vec{E} \cdot d\vec{l} \, d\psi + 2 \int \oint \vec{E}_v \cdot d\vec{l} \, d\psi. \tag{7}$$

The subscript v refers to the reference vacuum fields and fluxes with the same $\vec{B} \cdot \hat{n}$ and $\vec{E} \times \hat{n}$ boundary conditions as when the plasma is present. In Eqs.(6) and (7), the first term is just the resistive dissipation of helicity within the plasma. Without loss of generality, the plasma dissipation term can be replaced by $-K/\tau_K$, where τ_K represents the global decay time of the helicity. The second term represents helicity injection. Often, as shown below in Sec.II, the structure of the vacuum fields is obvious, and the helicity injection rate is easily computed. It should be noted that a steady state (sustainment) can be achieved where the helicity dissipation by the plasma resistivity is balanced by helicity injection.

Finally, it is useful to cast the plasma helicity dissipation in terms of the plasma resistivity. Ohm's law can be written as[21]

$$\vec{E} + \vec{v} \times \vec{B} + \vec{c} = \eta \vec{J}, \tag{8}$$

where $\vec{c}$ incorporates all the terms normally neglected in single-fluid MHD. Taking the scalar product of Eq.(8) with $\vec{B}$, integrating over the volume, and using Taylor's hypothesis ($\int \vec{c} \cdot \vec{B} \, dvol \approx 0$), it is apparent that helicity dissipation

$$\int \vec{E} \cdot B \, dvol = \int \eta \vec{J} \cdot \vec{B} \, dvol \tag{9}$$

occurs only from ohmic dissipation (from true electron collisional resistivity).[11,22]

II. Formation and sustainment

Five different methods of spheromak formation have been used, namely, the magnetized coaxial source,[23–25] the combined θ-pinch and z-pinch,[15] the flux core,[26] the conical θ-pinch,[27] and the kinked z-pinch[28] ($m = 1$ source). The initial spheromak formation experiments (the z, θ-pinch at Maryland, and the coaxial sources at Los Alamos and Livermore) were conceived and executed as "fast" formation schemes. The formation occurred in a period similar to the Alvén transit time (which required high electrical power), and the currents were carefully programmed to allow the necessary magnetic reconnection to take place. Even the then slower (magnetic reconnection timescales) flux core method was executed on the basis of detailed MHD calculations.[26] Since that period, spheromak formation has been understood and improved on the basis of helicity balance. It has been showed that these plasma sources are also helicity sources (Eqs.(6) and (7)), and that the helicity produced is injected and incorporated into the spheromak equilibrium in timescales much shorter than the resistive decay time.[4,2] Moreover, it has been shown that the helicity injection can be maintained indefinitely to balance the resistive helicity dissipation and to sustain the spheromak.[29]

The generality of the helicity injection model, independent of the formation details, has been firmly established. A source with $m = 0$ symmetry (coaxial gun) has been used to sustain an equilibrium with $m = 1$ symmetry.[16] The coaxial gun has also sustained flipped spheromaks, in which the outer spheromak poloidal field cannot simply connect to the gun electrodes.[4] In addition, a helicity source with $m = 1$ symmetry (kinked z-pinch) has sustained spheromaks ($m = 0$ symmetry),[12] also a case in which no simple connection of the spheromak flux to the source electrodes is possible.

Pioneering work by Alfvén involved the injection of plasma rings produced by a magnetized coaxial source into vessels bounded by insulating walls to study astrophysical phenomena.[30] These objects had the magnetic axis outside the wall, and thus are not spheromaks. However, "flux amplification" (toroidal-poloidal flux conversion by relaxation processes) was observed,[31] just as in CTX.[4] Also, Wells injected "plasmoids" with magnetic helicity produced by a conical θ pinch into a vessel with insulated walls.[32] But again, with no metallic wall to confine the helicity, the magnetic axis was outside the wall, and the equilibrium inside the vessel was not a spheromak.

A. Coaxial gun source

Fig.1 illustrates the coaxial-gun spheromak-formation method. The source is connected to the spheromak flux conserver wall by a cylinder with conducting walls called the entrance region. The source center electrode contains a solenoid which is energized prior to the discharge, to produce a magnetic flux ϕ_{src} which links the inner and outer electrodes. The outer electrode is generally electrically grounded, although it could in principle be energized. A gas puff is introduced into the inter-electrode gap, and once the gas has diffused enough, a voltage V_{src} between the electrodes is applied. The gas breaks down, and a radial current I_{src} (current density $\vec{J}_{src}$) between the electrodes is established. This radial current produces an azimuthal magnetic flux (magnetic field $\vec{B}_\theta$). The linkage of the azimuthal flux (produced at a rate V_{src}) arising from the radial current with the initial solenoidal flux constitutes the helicity generated by the source. When the source current is sufficiently large, $\vec{J}_{src} \times \vec{B}_\theta$ exceeds the restoring force of ϕ_{src}, the

equilibrium expands into the flux conserver and relaxes into a spheromak configuration within a few microseconds. More generally, the characteristic size of the driven equilibrium at the source is $\lambda_{src} = \mu_0 I_{src}/\phi_{src}$. When $1/\lambda_{src}$ decreases below the characteristic size of a possible equilibrium at the entrance region, the helicity flows "down-hill" in λ,[12] and the energy is minimized by the establishment of a spheromak equilibrium at the flux conserver, the volume of largest characteristic size.

The final spheromak helicity content can be predicted using Eq.(7). For the coaxial source, the reference vacuum magnetic field is simply the solenoidal field, and the reference electric field is simply due to the voltage applied between the electrodes. The resulting electrostatic helicity injection rate is then $2V_{src}\phi_{src}$. This result is easily understood by noting that for two simply linked tubes of flux ϕ_1 and ϕ_2, the magnetic helicity is $K = 2\phi_1\phi_2$.[1] In the coaxial gun, V_{src} is the production rate of azimuthal flux, which is linked by the invariant solenoidal flux ϕ_{src}. Thus $\dot{K} = 2V_{src}\phi_{src}$ is the rate of electrostatic helicity production. The evolution of the spheromak helicity content is[4]

$$\frac{dK}{dt} = \frac{-K}{\tau_K} + 2V_{src}\phi_{src}, \tag{10}$$

where τ_K is a function of the plasma resistivity and λ. For continuous injection (the configuration in Fig.1b is maintained), the spheromak fields reach a steady state value where dissipation balances injection, and relaxation distributes the current drive to maintain the spheromak near the minimum energy state. Once the V_{src} is turned off, the spheromak fields disconnect from the source and freely decay resistively (Fig.1c). The helicity balance in the CTX spheromak has been verified experimentally.[4] It has been verified also that spheromak sustainment by helicity injection (at spheromak currents of up to 500 kA, limited by the available Volt-seconds in the capacitor bank) can proceed for times much longer than τ_K.[29,4,33]

Sustained CTX spheromaks which are clean (power balance not dominated by radiative losses) have been obtained.[22] Therefore, current-carrying electrode-plasma contacts do not appear to be an important technological hurdle. Coaxial sources could prove to be a simple, inexpensive current-drive mechanism for a fusion reactor, not only for spheromaks, but for tokamaks and RFPs as well. In fact, helicity injection with a coaxial source has been demonstrated in a tokamak,[34] and a tokamak with start-up and current-drive provided exclusively by a coaxial plasma gun[35] is under construction at the Univ. of Washington. A spheromak reactor design based on a coaxial plasma gun has also been done.[36]

Although coaxial plasma guns have proven remarkably robust as spheromak sources, it is important to understand the physical processes which determine their performance, particularly when efficient operation is required for larger experiments. Although the literature on plasma guns is quite extensive, recent progress has been achieved in the MHD modeling of guns as spheromak sources.[37]

B. Theta-z pinch

Fig.2 illustrates spheromak formation with combined θ and z pinches.2 Starting with a static gas fill, an axial magnetic field is produced by the θ coil, and an axial voltage V_{src} is connected across the axial electrodes, which ionizes the plasma and draws an axial current. Defining the bias axial flux linking the electrodes as ϕ_{src}, the helicity injection

rate is again $2V_{src}\phi_{src}$. The current in the θ coil is reversed, and the reversed external bias field pinches the plasma and trapped initial bias flux towards the axis. The axial fields then reconnect, and the spheromak is formed. No measurements have been done of how much reverse axial flux links the axial electrodes (which would decrease or even reverse the helicity injection rate).

This method could be used in steady state, provided the reverse bias was limited (to maintain some net flux linking the electrodes along the direction of the initial bias field trapped near the axis). Maintaining the voltage between the electrodes would maintain helicity injection. This configuration corresponds to the "Bumpy z-pinch".[38] This configuration has been successfully achieved by the spheromak group at the University of Tokyo[39] by replacing the z-pinch electrodes by opposing plasma guns.

C. Flux core

Back when both the θ-z-pinch and gun formation methods were operated in the fast mode, the spheromak group at Princeton proposed a formation method based on an annular flux core,[26] which operates on the slower magnetic reconnection timescale. The core, which is covered by a resistive metal liner to allow flux penetration, contains both a toroidal solenoid (TF coil) to provide an azimuthal field, and a multi-turn azimuthal coil (PF coil) which produces a poloidal field surrounding the core. This method is depicted in Fig.3. The linkage of the poloidal and toroidal fluxes produced by the core are the basis for helicity injection in this scheme. This method, which precedes the present understanding of spheromak formation in terms of helicity injection, was based on extensive resistive MHD simulations which included magnetic reconnection processes.[26]

The formation proceeds as follows. In the presence of a gas fill, a bias vertical field along the axis of the core is turned on. Then the PF coil is energized to produce a poloidal field linking the core, in a direction which opposes the vertical field at the axis. The TF coil is then energized, the $d\phi_{TF}/dt$ induces a poloidal electric field around the flux core, and the plasma breaks down. The plasma ends up with toroidal field which opposes the toroidal field inside the core. This field drives the plasma towards the magnetic axis, where the poloidal field is weakest. Meanwhile, the PF coil current is ringing down towards zero, which induces an increasing toroidal current. As in the θ-z-pinch case, as the PF coil current drops towards reversal, the initial poloidal flux linking the magnetic axis reconnects outside the magnetic axis. The final poloidal field near the core ends up compressing the spheromak and the initial bias flux ends up surrounding the spheromak.

In this case, the helicity injection rate is again $2V_{src}\phi_{src}$, where ϕ_{src} is the flux produced by the PF coil, and $V_{src} = d\phi_{TF}/dt$. This method intends to avoid current-carrying contacts to the walls. However, the flux core is not in practice a flux surface, so the non-electrode advantage has not been realized. In principle, proper programming of the TF coil should allow a precise control of the spheromak profiles. In practice, early during formation, the profiles quickly relax to the minimum-energy state.[40-42] Fig.4 shows the spheromak magnetic profile evolution in S-1.

In principle, oscillating currents in the PF and TF coils in the flux core could be used for steady-state AC helicity injection into a spheromak,[43] akin to the F-θ pumping technique in RFPs.[44] However (with the benefit of hindsight), because of instability of non line-tied spheromaks without a conducting wall (see Sec.IV.A) and the relative technical difficulty of the flux core formation method, it is unlikely this scheme would be the

preferred choice for future devices.

D. Kinked z-pinch (m=1 source)

Another electrostatic helicity injection method is the use of a z-pinch with axial flux.[28,12] The experiment is shown in Fig.5. The basis for helicity injection is the linkage of the initial bias magnetic flux ϕ_{src} along the z-pinch axis with the magnetic flux due to the axial pinch current, driven by the voltage $2V_{src}$ between the electrodes (the vacuum vessel is grounded, and the electrodes are biased to $\pm V_{src}$ relative to ground). The helicity injection rate is then $4V_{src}\phi_{src}$. Possible advantages of this method include a better coupling of the source with an $m = 1$ state in the entrance region, which is the minimum energy state for that subvolume. This could decrease the relaxation drive (and associated loss of magnetic energy) in the entrance region. In addition, the source impedance turned out to be significantly higher,[12] an attractive technological feature. In addition, if no electrodes are allowed, the linear z-pinch can be replaced by a toroidal z-pinch driven by a transformer. A possible disadvantage is that the $m = 1$ structure in the entrance region can intrude into the spheromak flux conserver, causing stochasticity.[12]

III. Equilibrium

The achievement of magnetic field profiles corresponding to the spheromak configuration was verified in early experiments by internal magnetic probe measurements,[15,26,2,29] all showing the required signatures of poloidal field reversal at the magnetic axis, toroidal field reversal at the geometric axis, and similar toroidal and poloidal magnetic flux magnitudes. Fig.6 shows the magnetic-field profiles from the Beta II experiment,[2] which match extremely well those of the minimum-energy configuration. On the theory side, spheromak equilibria can be computed whether the boundary is a conducting wall or an external bias magnetic field. Analytic solutions have been obtained for equilibria in which a conducting sphere contains a concentric shell filled by a force-free magnet, inside which there is a compact torus equilibrium.[45] Analytic solutions for the minimum energy spheromak MHD equilibrium have been obtained in a spherical[46] and cylindrical[14,47] geometries. In other geometries, the equilibrium is found by solving the Grad-Shafranov equation, with the poloidal flux as a free parameter determining the absolute field strength of the equilibrium. In addition to specifying the boundary conditions, either $p(\psi)$ and $\phi(\psi)$; or $p(\psi)$ and $\lambda(\psi)$ must be specified, where ψ is the normalized poloidal flux function, $p(\psi)$ is the pressure profile, and $\phi(\psi)$ is the normalized toroidal flux function. For the minimum-energy state ($p(\psi) = 0$ and $\lambda(\psi)$ =constant), if the boundary is chosen to be a magnetic flux surface, the geometry of the boundary determines the magnetic field profile.

Radiation-dominated spheromaks are not likely to deviate far from the minimum-energy state. In radiation-dominated plasmas, the plasma resistivity tends to be spatially constant because as the electron temperature rises, the increase in Spitzer resistivity from the increased Z_{eff} partially offsets the decrease from $T_e^{-3/2}$. It has been shown that a minimum-energy spheromak with uniform resistivity decays self-similarly with a decay time $\tau_{B^2} = \mu_0/2\eta\lambda^2$ and remains in that state without assistance from relaxation processes.[48] In addition, a decaying spheromak with uniform resistivity initially not in the minimum-energy state evolves towards the minimum-energy state.[49,50] As expected, cold spheromak profiles are usually found to be very close to the minimum-energy

state.[48,2,42,27]

Spheromaks with higher electron temperatures and better impurity control[51,3,52] exhibit higher resistivity gradients, which cause the $\lambda(\psi)$ profile to deviate from the minimum-energy state. Deviations from the minimum-energy state due to higher edge resistivity are also observed in RFPs.[11] In decaying spheromaks, a signature of these deviations is the observation of internal current-driven ideal kink modes,[3,53] which are unstable for sufficiently large deviations from $\lambda(\psi) = constant$ (see Sec.IV.B). Current-driven modes are also observed because of non-uniform $\lambda(\psi)$ profiles induced by the formation[41] sustainment processes.[54]

In achieving clean spheromaks with higher electron temperatures, internal magnetic-probe measurements are a liability. The fitting of data from magnetic probes at the plasma boundary (or equivalently, the measurement of the induced currents in the conducting wall) to the results from a computer code which solves Grad-Shafranov equilibria has been successfully used to model spheromak equilibria in CTX.[5] For the (relatively low β) CTX spheromaks in mesh flux conservers (MFC), the electron pressure profile (determined from Thomson scattering and well approximated by $p(\psi) \propto \psi^n$ with $1 < n < 2$) is found to make little difference in the computed equilibrium fields. Although surface magnetic fields at the boundary do not uniquely determine the equilibrium, the CTX MFC data is well fitted by equilibria calculated from a physically reasonable linear $\lambda(\psi)$ function[3] given by $\lambda(\psi) = \bar{\lambda}[1 + \alpha(2\psi - 1)]$, where $\bar{\lambda} = \int \lambda(\psi)\, d\psi$ is the average $\lambda(\psi)$, usually very close to λ_{me}. Fig.7 illustrates the evolution of the $\lambda(\psi)$ slope α for a typical CTX large (0.67 m radius) MFC discharge During sustainment, the current profile (and equivalently the $\lambda(\psi)$ profile) is peaked on the outside due to source-driven currents on the outer flux surfaces. The safety factor q near the magnetic axis reaches unity, and the n=1 kink mode is observed. When the helicity source is turned off, the higher plasma resistivity at the outer flux surfaces causes the current at the outer flux surfaces to decay faster, and the current profile becomes peaked at the magnetic axis. The q near the magnetic axis decreases to 1/2, and the n=2 kink mode becomes unstable. Sometimes, further peaking occurs and the n=3 mode is observed. In spite of the seemingly large deviations of the $\lambda(\psi)$ profiles from those of the minimum-energy state, the magnetic energy of these spheromaks is less than 10% above that of the minimum-energy state with the same magnetic helicity content.[3]

There is evidence that during spheromak formation and sustainment, relaxation processes, which drive the spheromak equilibrium back towards the minimum-energy state, are present and responsible for incorporating the source helicity into the spheromak equilibrium.[41,4] Similarly, there is evidence that deviations from the minimum-energy state in CTX MFC decaying discharges due to resistivity gradients are countered by relaxation processes responsible for poloidal current-drive at the resistive spheromak edge (or equivalently, poloidal to toroidal flux conversion) which maintain the spheromak near the minimum-energy state[55,21] (see Sec.V.B).

IV. Stability

Spheromak stability can be discussed under three general topics. The first is external current-driven modes (tilt and shift modes), which occur when the spheromak is bounded by a vertical field, and there is no nearby conducting wall. (This case includes steady-state spheromaks inside a non-superconducting metallic wall.) The second is internal

current-driven modes, which have been mentioned in Sec.III. The third is pressure-driven modes.

A. External current-driven modes

It has been shown analytically that a spheromak in a uniform bias magnetic field is unstable to the tilt,[46] with a growth time of a few Alvén times.[14,47,56-58] In simple terms, the magnetic moment of the spheromak opposes the bias field and tends to flip.[59] The tilt in the presence of a bias flux is a relaxation process which conserves helicity. Initially, the spheromak toroidal flux does not link the bias field (no contribution to helicity). Once the spheromak flips, the bias field nibbles away at the spheromak poloidal flux.[57] If the bias flux is larger than the spheromak poloidal flux, the spheromak is destroyed. Otherwise, the bias flux is trapped near the spheromak geometric axis. The linkage of the toroidal flux with the combined bias and remaining spheromak poloidal fluxes yields the same initial helicity (if helicity dissipation is neglected for the duration of the process).

The presence of a conducting wall sufficiently close to the separatrix provides the image currents necessary to stabilize the tilt and shift modes,[46,14,47,59] provided the spheromak boundary is sufficiently oblate. This fact has been verified experimentally.[24,2] For both modes, these image currents have sizable components along the poloidal direction.[59]

If the bias field is made mirror-like with a high enough curvature index ($n_i > 1$, where $n_i \equiv (-r/B_z)(\partial B_z/\partial r)$), the tilt is stabilized, but the spheromak is then unstable to the horizontal shift mode, because the spheromak tends to move to regions of lower field.[59] For $n_i < 0$ the shift is stable (but the tilt is not), and for $0 < n_i < 1$ both the tilt and the shift are unstable.[59] Thus, a steady state spheromak reactor appears to need feedback stabilization, but the presence of a sufficiently conducting wall near the separatrix would decrease the needed response-time of the circuit to an acceptable level.

Stabilization of the tilt and shift modes has been attempted using passive coils rather than full conducting shells. One motivation has been that a conducting shell near the spheromak separatrix is incompatible with the flux-core and the traditional θ-z-pinch formation methods. Using a current loop model,[59] it has been predicted that properly placed figure-8 coils can stabilize both modes simultaneously (for times short compared to the L/R time of the coils) provided n_i is close to unity.[60] Besides the possible discrepancies in applying this model to spheromaks (normally low aspect ratio tori), it is difficult with simple coil sets to maintain a uniform field index throughout the spheromak cross section. In fact, it was difficult to maintain an index above zero on ProtoS-1/C without interfering with the formation process.[61]

It has been found computationally that line tying slows the growth rate of the tilt mode.[62] However, for realistic plasma parameters, line tying alone cannot completely suppress the tilt.[61]

Initial short-lifetime spheromak experiments, using various combinations of figure-8 coils, saddle coils, and resistive liners, sufficiently slowed the tilt and shift modes to prevent a catastrophic end to the plasma.[63-65] Additional methods, such as "wagon wheel" and solid metal plates have been tested in ProtoS-1/C. These methods have been effective only to the extent that line-tying has been present (for example, a copper plate allows a much faster growth rate than a thin stainless-steel wall does).[61] The fact that these tilt-limited spheromak lifetimes match the lifetimes in ProtoS-1/C with figure-8 and saddle coils,[61] suggests that previous experiments with figure-8 and saddle coils

benefited significantly from line-tying effects. "Wagon wheel" spokes connected poloidally around the outside of the ProtoS-1/C flux core significantly decreased the growth rate, but effectively acted like a conducting wall too far away from the separatrix to completely stabilize the tilt.[61]

Stabilizing schemes other than a close-fitting conducting wall have not successfully suppressed the tilt and shift modes in larger experiments with stationary spheromaks. With the figure-8 system, S-1 was grossly unstable with less than 10% spheromak poloidal flux linking the flux core.[40] In S-1, enough stability to study energy confinement has only been possible by the use of a pair non-connected conducting funnels along the geometric axis on the top and bottom of the spheromak.[40] In the Maryland Spheromak (MS) experiment, Figure-8 coils, a conducting cylinder along the geometric axis, copper plates on top and bottom of the spheromak, and aluminum cones have been ineffective.[66] Even if these methods could be made to work, it has been shown that open field lines which intersect walls or a neutral gas fill are extremely detrimental to global energy confinement in spheromaks.[22,55,67] Thus it might be unproductive to pursue these approaches further.

The space between two long coaxial conducting cylinders is not capable of supporting a stable stationary spheromak (the $m = 1$ double helix is the minimum-energy state). However, stable spheromaks have been accelerated in just that configuration, in a scheme where the spheromak acts like a moving armature in a coaxial rail gun.[68] The acceleration is due to the toroidal flux generated behind the spheromak by current flow axially along the center electrode, radially along the spheromak surface, and back axially along the outer electrode. Fig.8 illustrates the experimental geometry of RACE.[68] Rings with a 10 to 1 ratio of kinetic to internal magnetic energy have been compressed by focusing into a section of decreasing radius (conically shaped) where the spheromak either reflects back or stagnates.[68] Spheromak translation might allow tokamak plasma refueling by injecting spheromaks deep enough into the tokamak plasma before the spheromak unravels in the tokamak magnetic fields,[69] as demonstrated in the ENCORE tokamak.[34]

B. Internal current-driven modes

The observation of these modes has been described above (see Sec.III). These modes have been found to saturate at amplitudes of about 10%.[3] It has been predicted that these non-resonant modes should be present for sufficiently large deviations from the uniform λ profile,[70] and that they should saturate at about the observed amplitude, where the plasma should settle into a new equilibrium including the helical distortion from the mode.[71] The prediction is that with finite resistivity, since there are no singular current densities in the saturated state, there should be no rapid reconnection processes such as those associated with sawteeth in tokamaks.[71] Although this statement often holds true experimentally, sawteeth-like oscillations have been seen in sustained CTX spheromaks.[33] The expectation is that other than helical deformations to the flux surfaces, these internal kinks should have little effect in plasma confinement.

Experimentally, the non-uniform $\lambda(\psi)$ profile that drives the kinks is induced either by the formation and sustainment process,[41,3] or by the higher edge resistivity in decaying spheromaks.[3] These internal kinks are sometimes very damaging, and sometimes inconsequential. In detached S-1 spheromaks, a single n=2 kink event has destroyed energy confinement.[72,91] In decaying CTX discharges in the large MFC, the n=2 sat-

urated kink mode degraded particle confinement.[22] But since energy balance was not dominated by particle convection losses, no effect was seen in the energy confinement.[22] In the 0.6 m radius solid flux conserver (SFC) in CTX, the best energy confinement times of any spheromak have been obtained in the presence of the usual $\delta B/B \approx 10\%$ saturated level at the wall from the n=2 kink.

Sometimes, these modes can result in stochastic field lines which degrade confinement. In the $m = 1$ source experiment, the resonance between the $m = 0$ equilibrium and the large $m = 1$ distortion in the spheromak probably resulted in significant stochasticity.[12] In high current-density spheromaks in the 0.3 m radius solid flux conserver (SSFC), there is apparently significant stochasticity arising from the interaction of the saturated n=2 kink with toroidal distortions of the flux conserver,[73] which results in degraded confinement and τ_{B^2}.

C. Pressure-driven modes

The volume-averaged beta-limit β_c given by the Mercier criterion for a spheromak in a spherical boundary is a very low 0.2%, while for oblate spheromaks, $\beta_c \approx 1\%$.[46,74–76] This is because the spheromak curvature is always unfavorable, and the shear of the magnetic field is very low.

There are ways to significantly increase shear in spheromaks. The presence of a sharp current and flux hole along the spheromak geometric axis can raise β_c to the 10–40% range, depending on the specific magnetic profiles and aspect ratios ($1.2 - \infty$) studied.[46,74,75,70] Sufficiently peaked $\lambda(\psi)$ profiles can also raise β_c significantly above 2%.[46,70,76] More recently, it has been determined that modifying the shape of a cylindrically symmetric wall to have a "bowtie"-shaped cross section can raise β_c to 3% for spheromaks in the minimum energy state, and higher for the outwardly peaked $\lambda(\psi)$ profiles typical with coaxial gun sustainment.[77] Fig.9 shows the geometry of this configuration.

For ideal interchange modes, the Mercier limit is probably a conservative limit. Unless the criterion is significantly violated, the growth rates are so small that resistivity, viscosity and kinetic effects would probably dominate ideal MHD effects.[75] Resistive pressure-driven modes are a potential problem,[46,70] but they have not been identified in spheromaks. Should pressure-driven modes represent the ultimate limit to spheromak confinement, a "constant-β" scaling would be expected.

Initial spheromak experiments reported volume-averaged betas $\langle\beta\rangle_{vol}$ much above β_c, of up to tens of percent.[15,26,63,64,78,79,51,54,80,40,81] In more recent S-1 discharges, a local constant β scaling has been found at the magnetic axis.[67] However, similarly to CTX spheromaks in the large MFC, the $\langle\beta\rangle_{vol}$ has decreased from previous values, but for reasons unrelated to pressure-driven modes.[22,67] The more recent CTCC-II experiment at Osaka has obtained a $\langle\beta\rangle_{vol}$ of a few percent.[82] But because of limiters, CTCC-II has a current hole,[82] thus its β_c should be higher. CTX spheromaks in the high current density SSFC show no evidence of pressure-driven instability, even though $\langle\beta\rangle_{vol} \approx 5\%$.[73]

In decaying CTX spheromaks in the SFC, a pressure-driven interchange mode has been directly observed.[83] Even though $\beta_c \approx 0.5\%$ when the instability occurred, the electron density and temperature (from Multipoint Thomson scattering) and the assumption of equal electron and ion temperatures (substantiated by Doppler broadening measurements of OV^{85}) yield an actual $\langle\beta\rangle_{vol} \approx 5\%$.[83] During the decay of these discharges, the

electron pressure profile continually peaked, until, when a critical pressure gradient was reached, the interchange occurred. But the electron pressure gradients were so large, that the critical gradient from the Mercier criterion (using the linear $\lambda(\psi)$ profile fit to the magnetic probe data) was exceeded by a factor of 20 by the electron pressure alone.[83] Fig.10 shows the SFC geometry. Fig.11 illustrates the nature of the instability. The magnetic diagnostics showed no signature associated with the interchange, as expected for this type of mode.

Since the nature of the observed violations of the Mercier criterion in spheromaks is not known, it is probably optimistic to expect them to hold as more reactor-relevant conditions are approached. However, even if current holes or $\lambda(\psi)$ profile control should prove difficult, the use of a bowtie-shaped flux conserver represents a simple way of achieving a very useful β, while retaining the engineering advantages of the spheromak concept.

V. Confinement

A. Early work

Because of the variety of spheromak formation schemes, it is traditional to compare spheromak confinement in the decaying phase, when the spheromak fields are not being sustained by helicity injection, the spheromak has mostly disconnected from the source, and the formation details should make little intrinsic difference. Although some confinement data for sustained spheromaks is available (and not dramatically different from that of decaying spheromaks),[22] this paper discusses only the overwhelming body of data from decaying discharges. For the relatively short (compared to τ_{B^2}) energy confinement times τ_E in most spheromak experiments. the steady state approximation

$$\tau_E = \frac{3}{2}\langle\beta\rangle_{vol}\,\tau_{B^2} \tag{11}$$

can be used. With Eq.(11) as a model, the β and τ_{B^2} will be separately discussed in Secs.V.B and V.C.

In early spheromak experiments, the dominant plasma loss mechanism and the limit to plasma electron temperature was impurity radiation.[83] The Maryland and Princeton spheromak groups had the expectation that, once their gross stability problems were solved with loosely fitting conductors or a conducting center rod, the relatively small plasma-wall contact area (including the lack of electrodes for spheromak formation) would allow the achievement of excellent plasma confinement in their experiments.[83] Meanwhile, the CTX group at Los Alamos, realizing that impurity radiation was dominating energy transport, decided to switch to a 0.4 m radius flux conserver constructed out of a mesh of copper bars (SMFC), to minimize the wall surface area in contact with the plasma and to allow the rapid "pump-out" of impurities out of the plasma.[51] In retrospect, for reasons explained in Secs.V.B and V.D, both strategies were fatally flawed, because of the disastrous effects of open field lines in force-free concepts, much beyond those in other concepts. Only the group at Osaka used the combination of technologies that could significantly advance spheromak research in the short term: solid flux conservers and titanium gettering for impurity control.[52] However, because of the lack of some key diagnostics and their understandable preoccupation with pressure-driven

modes (from theoretical considerations), the importance of their results and technology was missed within the spheromak community.

These strategies of wall-contact minimization for a while appeared to be working. In the CTX SMFC, an electron temperature of 100 eV was achieved for the first time in any spheromak.[51] The power balance in the SMFC was dominated by power losses from particle convection.[80] However, in spite of the higher temperatures, no increase in energy confinement times (relative to previous results in solid flux conservers[79]) was obtained, because of an increased helicity decay time.[51] These problems came to a dramatic focus when the large MFC was installed in CTX. It was found that in spite of large increases in magnetic field and toroidal plasma current (up to 1 MA) along with similar plasma and current densities, the resistive decay time remained independent of the core electron temperature, the energy confinement time did not improve, and $\langle\beta\rangle_{vol}$ actually dropped as R^2.[22] Similar results on the global plasma confinement properties were measured in S-1.[67]

B. Helicity dissipation

In nearly force-free configurations, relaxation processes tend to dispose of the magnetic energy while conserving magnetic helicity. Magnetic helicity K is dissipated ohmically (through electron collisional resistance). So a productive approach is to examine first the determinants of helicity dissipation. If $\lambda(\psi)$ gradients are not present, then there is simply a proportional decay of the magnetic energy W (Eq.(4)). However, if $\lambda(\psi)$ is non-uniform, then magnetic energy and helicity are not dissipated at the same rates, and relaxation activity is possible. This fact, and its consequences for energy transport, is what makes the behavior of force-free configurations unique.

Non-radiation-dominated spheromaks with significant fractions of open magnetic flux had helicity decay rates much higher than predicted by the volume-averaged Spitzer resistivity.[22,67] This is because the global plasma resistance was dominated by the electron-neutral collisions at the spheromak edge, rather than by the lower Spitzer resistivity anywhere including the edge.[22,67]

The dissipation of helicity under this situation of high resistivity from neutrals is described here using CTX spheromaks in the large MFC. Fig.12 shows a diagram of the large MFC, along with the poloidal flux surfaces, determined from the surface currents measurements in the MFC fitted to the MHD equilibrium model,[3] but this time accounting for the discreteness and finite conductivity of the mesh copper bars.[22,55] Because of the competition of effects such as current peaking into and field diffusion out of the flux conserver, the open fraction of poloidal flux remains a nearly constant 25% throughout the decay phase. The plasma in the open field lines leaves fast. Without refueling, there develops a severe shortage of current carriers, and if unchecked, the edge plasma currents would simply die out, and the spheromak would turn into a field-reversed configuration (FRC) with nearly only toroidal current. This configuration is so far from the minimum-energy state, that strong relaxation activity attempts to drive edge plasma currents. But since the edge becomes nearly an insulator, $\eta\vec{J}$ grows without bound. From Eq.(7), the helicity dissipation rate also grows and the spheromak quickly dies.[55,22,70]

The spheromak lifetime can be extended by refueling the edge with a background hydrogen fill.[70] In that case, the voltage on the open poloidal field lines is limited to the Paschen breakdown voltage for hydrogen.[84] This is indeed observed in the large

MFC discharges with the presence of a neutral hydrogen fill.[22] Fig.13 shows the good agreement between: (a) A plot of the observed E_{eff} (which is $\approx \eta \vec{J}$ at the edge, as determined from helicity balance), versus the electron density n_e (which is proportional to the neutral fill pressure[79]); and (b) The corresponding Paschen curve for breakdown of hydrogen.[22] A posteriori, it is evident that the helicity dissipation in the open flux from the electron-neutral resistivity is enough to account for the total spheromak helicity dissipation, so that the dissipation from the Spitzer resistivity at the plasma core can be neglected to within experimental uncertainty.[25] Because of this, a plot of core electron temperature versus τ_{B^2} yields no correlation whatsoever in both CTX with the large MFC and S-1.[22,67] This model is similar to the edge-helicity-dissipation model pioneered in the HBTX RFP.[20]

The ideal situation is not to need neutrals at the edge, so that plasma resistance is dominated by Spitzer resistivity, with τ_{B^2} increasing as the plasma temperature increases. This situation has been achieved in decaying spheromaks in the CTX SFC before the onset of the pressure-driven mode by means of the combination of a low-field-error design of the flux conserver with Ti gettering for impurity control.[83,85] Fig.14, a plot of τ_{B^2} versus central electron temperature in the SFC, shows for the first time in a spheromak a positive correlation between these quantities.[85]

Another thing learned from the edge-helicity-dissipation model is that the strong relaxation edge-current-drive (and corresponding anti-drive at the magnetic axis) observed in decaying spheromaks in the large MFC is due to effects beyond those included in single-fluid MHD.[21] This is in contrast with MHD dynamo mechanisms proposed for the spheromak and the RFP based on $\delta\vec{v}$ and $\delta\vec{B}$ fluctuations.[1,55,67,86] In RFPs, self-consistent single-fluid MHD calculations of the dynamo do not reproduce the observed magnetic fluctuation amplitudes.[87] The reason that single-fluid MHD does not appear to contribute to relaxation current-drive in the large MFC can be visualized in CTX by examining Fig.12 and Eq.(8). Consider (see Fig.12) a path following an open poloidal field line at the edge, which is closed along a (highly conducting) MFC poloidal copper bar. We examine the scalar product of Eq.(8) with the actual $\vec{B}$ (not the equilibrium field!) at the edge, and examine each term at a time. The term $\vec{E}\cdot\vec{B}$ is known from the decay of the spheromak toroidal flux.[55,67] The term $(\vec{v}\times\vec{B})\cdot B$ identically vanishes in both an instantaneous and a time-averaged sense. On the right hand side of the equation, the term $\eta\vec{J}\cdot\vec{B}\approx E_{eff}$ is known from helicity balance coupled to the edge-helicity-dissipation model, as described above.[55,21] By now, we have exhausted the single-fluid MHD terms. The problem is that the observed $\eta\vec{J}\cdot\vec{B}\approx E_{eff}$ is up to three times higher than the observed $\vec{E}\cdot\vec{B}$.[55,21] Previous attempts to balance the two with the $\delta\vec{v}\times\delta\vec{B}$ term arising from fluctuations relies on incorrect time-averaging where cancelling terms of the same order are dropped.[21] Apparently, the non-single-fluid MHD term $\vec{e}\cdot\vec{B}$ is responsible for relaxation current drive in spheromaks and RFPs.

C. Plasma beta

Because of the fact that in a spheromak the internal magnetic fields are self-generated, a particular β value is much more useful than in other devices such as tokamaks and stellarators, where these fields are mostly generated by external coils. An important figure of merit is the engineering beta, $\beta_{eng}\equiv\langle\beta\rangle_{vol}/B^2_{wall}$. Whereas in a tokamak $\beta_{eng}/\langle\beta\rangle_{vol}\approx 1$, in a spheromak the typical ratio is in the 3–4 range.[79] Thus a $\langle\beta\rangle_{vol}\approx 5$ – 10% in a

spheromak yields an excellent β_{eng} as far as reactor design is concerned.

Presently, the most important issue in spheromak confinement research is understanding what determines the β limit in a spheromak. From the results in the CTX SFC, there is certainly a limit beyond which there is a catastrophic end to peaked plasma pressure profiles.[83] However, it is possible that at a lower β, higher order saturated modes could enhance energy transport, which might account for the constant-β-scaling observed in the core of the S-1 plasma.[67] In the CTX SFC, where before the interchange radiation dominates the energy transport as the plasma heats up, there is no evidence of such mode-induced transport.[85]

As discussed in Sec.C, $\langle\beta\rangle_{vol} \approx 5\%$ describes present experiments well. Though the Mercier criterion is greatly exceeded in present spheromak experiments, it is unclear whether it would become relevant at more reactor-relevant parameters. Although the β_c limit from the Mercier criterion can be raised to high values by modifying the flux conserver geometry, it is important to understand what the real limit is. For example, resistive modes might become more important than ideal modes in future experiments.

D. Power balance with large fraction of open flux

The deleterious effects to plasma confinement of field-errors have been observed in both the S-1 and CTX large MFC experiments.[22,67] It is clear that this regime of spheromak operation does not represent a favorable confinement scaling for future experiments.

As discussed in Sec.V.B, the best way to limit the dissipation of helicity in open field lines is by providing a neutral gas fill pressure. But even then, the results when the fraction of open flux is large are not satisfactory. Because of parallel heat conduction, the electron temperature in these open flux surfaces is low, allowing deep penetration of the neutral hydrogen used for refueling. Even though the mean free for neutrals into these plasmas is only a few cm, the process of multiple charge exchange is important[67] according to simulations for parameters relevant for S-1 and CTX. In this process, a cold neutral exchanges with a warm ion in the edge, and the resulting warm neutral penetrates deep into the core. This effect should have raised the ratio of neutral to electron densities from the 10^{-5} range (ignoring multiple exchanges) to the 10^{-2} range (when multiple exchanges are considered).[67] This fact is disastrous for spheromaks dominated by field errors, as explained below.

Because the ohmic dissipation rates for helicity and magnetic energy are $\dot{K} \propto \eta\vec{J}\cdot\vec{B}$ and $P_{ohm} \propto \eta\vec{J}\cdot\vec{J}$, the dissipation rates as a function of flux surface is[22]

$$2\mu_0\frac{dP_{ohm}}{d\psi} = \lambda(\psi)\, d\dot{K}/d\psi \tag{12}$$

(although helicity cannot be treated locally, its dissipation rate can be). Moreover, because of the applicability of the edge dissipation model, the integral of Eq.(12) over ψ yields globally

$$2\mu_0 P_{ohm} \approx \lambda(0)\, \dot{K}, \tag{13}$$

where $\lambda(0)$ is the value at the edge. But, as observed in S-1 and CTX, with strong relaxation activity,[22,21]

$$2\mu_0 W = \langle\lambda\rangle \dot{K} \tag{14}$$

where the term $(d\langle\lambda\rangle/dt)K$ is experimentally observed to be negligible, presumably due to strong relaxation activity. Thus the ratio of ohmic power to helicity dissipation is[22]

$$\frac{P_{ohm}}{\dot{K}} \approx \frac{\lambda(0)}{\langle\lambda\rangle} \tag{15}$$

with the balance $\dot{W} - P_{ohm}$ dissipated by relaxation.

As discussed in Sec.V.B, because of resistive decay of the edge currents in decaying spheromaks, the ratio $\lambda(0)/\langle\lambda\rangle$ can become small (even under the linear λ profile model[3]), so the power going to relaxation becomes dominant. Similarly in RFPs, it has been found that the "modified" Bessel function λ profiles (where the current goes to zero steeply at the edge) fit the data much better.[18] How well these profiles fit CTX data is a topic presently under study. If such profiles were present in the CTX large MFC, the power going to relaxation would have approached unity.[55]

The magnetic power which goes into relaxation, presumably via fluctuations which move plasma, apparently goes into ion heating. In both S-1 and the CTX large MFC, Doppler impurity ion temperatures T_D of hundreds of eV are measured, with typically $T_D/T_e \approx 4$.[55,67] If the bulk ion temperature is indeed that high, the importance of charge exchange losses becomes apparent. Both a zero-dimensional analysis[22] and a one-dimensional analysis indicates that charge exchange losses are both dominant and sufficient to explain the energy balance in both the CTX large MFC and S-1. In both machines, this regime results in very unfavorable global confinement scaling. At constant j/n, to avoid drift instabilities, it is observed: $\dot{I} = constant \longrightarrow \tau_K \propto JR^2$ (R is the spheromak size); electron temperature T_e in the core independent of J; $\langle\beta\rangle \propto 1/J$, and; τ_E independent of J.[22,67] Clearly, this is not the way to operate a spheromak.

Even if charge-exchange losses could be decreased, because of the presence of relaxation, the regime with a large fraction of open flux is not desirable. For example, in sustained spheromaks, where $\lambda(0)/\langle\lambda\rangle > 1$,[3] the ohmic power dominates. However, with the helicity source bias flux used in present experiments (to which the spheromak poloidal flux can connect), parallel thermal conduction can dispose of the heat. The ideal way to operate a spheromak in steady state is with a helicity source maintaining the edge currents to avoid excessive relaxation activity (and possible associated enhanced transport), but with a source bias flux of less than 1% of the spheromak poloidal flux to reduce parallel heat losses to acceptable levels.[36]

Field errors due to a mesh or loose-fitting wall is not the only problem. In the higher current density and electron temperature spheromaks in the CTX SSFC (with copper walls and no limiters), all the classic signatures of field errors (*e.g.*, linear current decay, higher Doppler ion than electron temperatures) are observed when the saturated n=2 kink mode is active.[73,88] Because of fabrication errors, the cylindrical walls of the SSFC are not exactly round. Apparently, the resonance between the n=2 mode and the perturbation induced by the wall creates a sufficiently high fraction of stochastic magnetic flux. Because of peak electron temperatures of up to 400 eV[73] and thus lower core plasma resistivity, the tolerable open flux fraction is less than in the MFC plasmas.

In both the ProtoS-1/C and the S-1 devices, the particle diffusion coefficient has been measured by using a spark discharge between carbon tips located near the spheromak magnetic axis.[89-91] In both ProtoS-1/C and S-1, it is found that $D_\perp \approx 5D_{bohm}$ fits the results well.[90,91] These measured diffusion coefficients have been found to correlate with

pressure gradients.[91] In addition, these coefficients, in the nearly constant electron density n_e discharges considered, are consistent with the expected scaling $\tau_p \propto 1/v_{i,th}$ (assuming $T_e \propto T_i$, where $v_{i,th}$ is the ion thermal speed) resulting from pressure-driven modes and the observed $n_e T_e \propto B^2$. However, the associated particle replacement power is negligible, so anomalous ion heating coupled with charge exchange losses dominate the S-1 energy balance.[67]

Even if the Bohm-like diffusion observed in S-1 is due to pressure-driven turbulence, the actual numerical values observed might be more characteristic of S-1 than of the intrinsic confinement limit in spheromaks. For example, in the CTX SFC described below, there is no gas fill pressure, so the refueling of the core plasma presumably ceases when the source is turned off. In the SFC, whereas $5D_{Bohm} \longrightarrow \tau_p \approx 400\mu$s particle confinement time of the core plasma, it is observed instead $\tau_p \approx 1.6$ ms.[83]

E. Power balance with small fraction of open flux

As discussed in Sec.V.B, spheromaks in the CTX SFC are the ones closest so far to the ideal error-field-free spheromak. The observation of more normal Doppler ion temperatures $T_D/T_e \approx 1$ indicates that most of the magnetic power ohmically heats the electrons.[85] The positive correlation of τ_{B^2} with peak T_e also supports this picture.[85] As a result, the highest global energy confinement time in any spheromak, $\tau_E = 0.2$ ms, has been obtained. This achievement, along with the results of the HBTX-1B results without limiters,[92] are the best illustration so far of the importance of the edge helicity-dissipation model in the design of experiments with nearly force-free equilibria.

Because of the strong (non-optimal) pressure peaking observed in the CTX SFC,[83] $\tau_{B^2} \propto T_e$ is obtained for the decay time,[85] which yields $\tau_E \propto \beta T_e$. With a more gentle temperature profile where the globally-averaged electron temperature is proportional to the peak temperature, $\tau_{B^2} \propto T_e^{3/2}$ and $\tau_E \propto \beta T_e^{3/2}$ could be obtained. This yields: (at constant electron density n_e) $T_e \propto \beta I^2/R^2$ and $\tau_E \propto \beta^{5/2} I^3/R$, or; (at constant drift parameter $J/n_e\sqrt{T_e}$) $T_e \propto \beta^2 I^2$, $n_e \propto 1/\beta R^2$, $\tau_E \propto \beta^4 I^3 R^2$ and $n_e \tau_E \propto \beta^3 I^3$. Along with the high β_{eng} properties of the spheromak, these scalings illustrate the attractiveness of the concept.

VI. Some ongoing spheromak projects

In spite of the spheromak attractiveness as a fusion reactor, there has been a decreasing worldwide research effort in spheromaks for magnetic fusion. In the United States, in the face of decreasing fusion budgets, the Office of Fusion Energy (OFE) is sponsoring only the MS experiment at the Univ. of Maryland, along with smaller efforts at the Univ. of California, Berkeley, and at the California Institute of Technology. In Japan, research is continuing, but no major upgrades of present experiments are contemplated. In the United Kingdom, the recently commissioned SPHEX experiment at the Univ. of Manchester Institute of Science and Technology is a welcome development.

Presently in the United States, substantial defense-related spheromak projects are being carried out at the Air Force Weapons Laboratory, and at the Lawrence Livermore and Los Alamos National Laboratories. Along with their particular missions, these defense-related projects are making important contributions to the advancement of spheromak physics in general.

A. Japan

1. TS-3, Univ. of Tokyo

The TS-3 group has recently modified their device to allow flexible magnetic helicity injection (and spheromak production) with an axial discharge between the outer electrodes of two opposed coaxial guns and/or with a z–θ discharge. An external bias field can also be used.

They have produced stable flux–core spheromaks FCS (also known as "bumpy z–pinches", see Sec.II.B).[39] The current hole in this configuration can modify the spheromak q–profile to increase magnetic shear and increase the β limit. The q–profile can be modified to the extent that it can resemble that of the ultra–low-q and tokamak configurations.

2. CTCC–II, Osaka Univ.

CTCC-II features helicity injection by a magnetized plasma gun into an ellipsoidal aluminum flux conserver. The combination of a "choking coil" and a stainless-steel entrance region allows current-limiting on the outer flux surfaces to produce a FCS.

CTCC–II discharges are known to have 7–12% β at the magnetic axis, as determined from Thomson scattering.[82] They now use an MHD equilibrium model, incorporating separate parallel and perpendicular pressures, which produces a significantly better fit to the experimentally measured magnetic profiles.[82]

3. FACT, Himeji Institute of Technology

This recently commissioned experiment attempts to combine electrostatic helicity injection from a magnetized plasma gun with inductive helicity injection and translation by means of a ramp-down in the current in the "flux-amplification" coil. The spheromak is finally injected into a cylindrical flux conserver. Inductive helicity injection has not been demonstrated yet, but spheromaks formed with electrostatic helicity injection have been produced and studied.[93]

B. United Kingdom

1. SPHEX, Univ. of Manchester Inst. of Science and Technology

SPHEX features magnetic helicity injection into a flux conserver designed to minimize the magnetic flux penetrating the solid wall (field errors) and the associated helicity losses. SPHEX has presented results which reproduce well some expected key features. These include magnetic profiles close to the minimum–energy state, the presence of rotating kink modes, and a gun current/flux ratio which must be exceeded to obtain plasma and helicity injection.[94] The surprising feature is the large current which enters the flux conserver wall opposite to the gun, probably caused by processes other than simple flux diffusion.[94]

C. United States

1. MARAUDER program, Weapons Lab., Kirtland US Air Force Base

The MARAUDER experiment (presently under construction) intends to form a spheromak with a 500 kJ bank driving a coaxial gun, and accelerate the spheromak with the 9 MJ Shiva Star bank. The aim is to achieve ultra-high directed energy and radiation.

Simulations of spheromak formation with the MACH2 code have been presented.[95] (MACH2 is a two–dimensional MHD code.) Their results explored the range of gun parameters which result (or do not result) in spheromak formation. A key feature identified is the need for sufficient mass density to allow a sufficiently high ratio of magnetic/kinetic energy, which in turn allows proper magnetic reconnection of the magnetic field.

2. RACE, Lawrence Livermore National Lab.

In the RACE experiment, a coaxial gun forms spheromaks (plasma rings) which are then accelerated along coaxial electrodes.[68] Rings have been generated with velocities of up to 3×10^8 cm/s, with kinetic energies of 40 kJ.[96] Stagnation of the rings against a copper plate has produced 2.7 kJ of soft X-rays, with a spectrum above 10 eV.[96] Focusing of the rings to about a third of the initial diameter has been demonstrated.[97] Design of the Compact Torus Accelerator (CTA) within the RACE program is proceeding.[97] CTA has potential, when scaled to high energies ($\approx$ 100 MJ), in fusion applications. These include radiation production for indirect ICF drive and magnetically-insulated, inertially-confined fusion (MICF).[97]

3. ENCORE, California Institute of Technology

The Caltech group has been experimenting with helicity and plasma injection from a coaxial gun into the ENCORE tokamak. They have done experiments in which they inject into the magnetized vacuum vessel (no plasma), and observed a resulting magnetic structure with m=1 symmetry.[34] In their experiments of injection into a tokamak discharge, they demonstrated toroidal current drive, with fast toroidal current increases of $\approx$ 30%.[34]

4. BCTX, Univ. California, Berkeley

In BCTX, a coaxial magnetized gun injects magnetic helicity and plasma into a spheromak flux conserver. The mesh flux conserver in use until recently has just been replaced by a solid flux conserver (similar to early CTX designs). The purpose of this experiment is to eventually test a 20–40 MW pulsed lower-hybrid spheromak heating scheme.[98]

Spheromak lifetimes of 100 μs have been achieved in the 0.7 m diameter mesh flux conserver. These spheromaks exhibit the expected m=1 kink instability, rotating at a high rate. Optimization of plasma parameters is proceeding. Plasma heating experiments await the completion of the 40 MW, 450 MHz RF source. The RF drive components are now in place.[98]

5. MS, Univ. Maryland

In MS, spheromak formation is achieved using the z–θ discharge method. The spheromak magnetic field structures have been mapped out in detail.[66] The plasma is asymmetric during formation, evolving into a tilt followed by rapid plasma loss. Asymmetries have attributed to the reversal field coils or feed connections to the I_z electrodes. As remedies for the tilt, a stainless steel liner and copper cones have been ineffective, while Figure–8 coils have slowed it down. Titanium gettering and Elkonite electrodes have been used to reduce impurity problems. Doppler broadening of OII, OIII, OIV indicate anomalously–high ion temperatures of about 30, 75, 90 eV, respectively.[99] HeII temperatures as high as 100 eV at the geometric axis have been measured. Strong visible and UV radiation has been observed surrounding the electrodes. Line–averaged electron density from a multichord interferometer has been obtained.[100] An observed larger particle inventory than that provided by the fully ionized fill indicates a large impurity influx. The measured particle confinement time is $\sim 95\ \mu$s. Results from a 0-D energy–balance code indicate that a reduction in impurity content is needed to get higher electron temperature.[100]

6. CTX and HESS, Los Alamos National Lab.

Presently, the CTX facility is aimed at producing clean, high magnetic–field spheromaks by helicity and plasma injection into a flux conserver with solid, highly conducting walls. Suitable spheromaks will be compressed by the wall, driven by high explosives (HE). Ultimately, the spheromak will be used as an energy transfer and switching medium for accelerating metal foils to hypervelocity. Fig.15 shows a simulation of spheromak dynamics (including spheromak resistive decay) in the presence of the compressing dome.[73] The spheromak stores energy during most of the compression cycle, releasing it to the projectile at time $t \approx 79\mu$s. Fig.16 shows the progress in inverting an aluminum dome intactly as necessary for this experiment.[101]

Thomson scattering, density interferometry, and B–field data from small, high B–field spheromaks have been obtained in the 0.3 m radius cylindrical flux conserver (SSFC).[73] The data shows T_e as high as 400 eV, n_e in the range of $3–8\times10^{14}$ cm^{-3}, and maximum internal B–field in the range of 2.2–2.6 T. The stability properties of the $n = 1$ and $n = 2$ modes during decay have also been studied. Bolometry, spectroscopy, and Doppler T_i data have also been obtained.[88] Radiation losses have been shown not to dominate, while impurity–line radiation behavior is consistent with the multi–hundred eV electron temperatures measured with Thomson scattering. Doppler T_i values increase during strong $n = 2$ kink activity, to values as high as 1 keV.

The High Explosives Spheromak Source (HESS) is an implementation of a scheme to generate helicity mechanically.[102] In HESS, an HE-driven cylindrical wall generates helicity by driving an initial solenoidal magnetic field into twisted grooves in an opposing concentric cylindrical wall. The mechanical twisting of the field lines generates the helicity. Fig.17 illustrates the helicity injection sequence.[103] This experiment is under construction. Meanwhile, the HE expansion of the inner core has been demonstrated, and further HE experiments to maximize cleanliness of the process are proceeding.

VII. Summary

The concepts of magnetic helicity generation and relaxation to minimum-energy force-free states have been successfully used as the basis for spheromak formation and sustainment. It appears that the relaxation processes which drive spheromaks towards the minimum-energy state are not describable by single-fluid MHD. Successful theoretical modeling includes the MHD equilibria and stability of current driven-modes. Gross pressure-driven modes have been observed, but at pressure gradients much higher than predictions from the Mercier criterion. It is of great importance to reconcile the discrepancy.

Once the importance of minimizing magnetic flux penetration into the spheromak wall is understood, the prescription for a stable compact steady-state fusion reactor based on the spheromak is straightforward. It consists of a spheromak in a cylindrically symmetric conducting flux conserver with a bowtie-shaped cross section, driven by a coaxial magnetized gun linking less than 1% of the spheromak poloidal flux, and a $\langle\beta\rangle_{vol} \approx 10\%$ (from the Mercier criterion).

In addition to the traditional magnetic fusion applications, spheromaks have proven to be a robust configuration which can be translated and compressed. This opens the door to additional applications, such as tokamak refueling, radiation sources, magnetically insulated inertial confinement fusion, mechanical helicity production, and energy storage and transfer to accelerate projectiles to high velocities.

Acknowledgments

The author acknowledges the assistance of Thomas Jarboe. His spheromak review paper (in preparation) provided a unique perspective and a wealth of references from the literature on spheromaks. The useful discussions with Robert Mayo and Fred Wysocki on many spheromak references are gratefully acknowledged.

References

[1]H. K. Moffat. *Magnetic Field Generation in Electrically Conducting Fluids*. Cambridge University Press, New York, 1978.

[2]W. C. Turner, G. C. Goldenbaum, E. H. A. Granneman, J. H. Hammer, C. W. Hartman, D. S. Prono, and J. Taska. Investigations of the magnetic structure and the decay of a plasma-gun-generated compact torus. *Physics of Fluids*, 26(7):1965, 1983.

[3]S. O. Knox, Cris W. Barnes, G. Marklin, T. R. Jarboe, I. Henins, H. W. Hoida, and B. L. Wright. Observations of spheromak equilibria which differ from the minimum energy state and have internal kink distortions. *Physical Review Letters*, 56(8):842, 1986.

[4]Cris W. Barnes, J. C. Fernández, I. Henins, H. W. Hoida, T. R. Jarboe, S. O. Knox, G. J. Marklin, and K. F. McKenna. Experimental determination of the conservation of magnetic helicity from the balance between source and spheromak. *Physics of Fluids*, 29(10):3415, 1986.

[5]Kurt F. Schoenberg, Ronald W. Moses, Jr., and Randy L. Hagenson. Plasma resistivity in the presence of a reversed-field pinch dynamo. *Physics of Fluids*, 27(7):1671, 1984.

[6]Mitchell A. Berger and George B. Field. The topological properties of magnetic helicity. *Journal of Fluid Mechanics*, 147:133, 1984.

[7]L. Woltjer. A theorem on force-free magnetic fields. *Proceedings of the National Academy of Sciences, USA*, 44(6):489, 1958.

[8]J. B. Taylor. Relaxation of toroidal plasma and generation of reverse magnetic fields. *Physical Review Letters*, 33(19):1139, 1974.

[9]J. B. Taylor. Relaxation of toroidal discharges to stable states and generation of reversed magnetic fields. In *Plasma Physics and Controlled Nuclear Fusion Research, 1974*, volume I, page 161. IAEA, Vienna, 1975. Proc. Vth International Conference, Tokyo.

[10]J. B. Taylor. Relaxation of toroidal discharges. In D. E. Evans, editor, *Pulsed High Beta Plasmas*, page 59. Pergamon Press, New York, 1976.

[11]J. B. Taylor. Relaxation and magnetic reconnection in plasmas. *Reviews of Modern Physics*, 58(3):741, 1986.

[12]J. C. Fernández, B. L. Wright, G. J. Marklin, D. A. Platts, and T. R. Jarboe. The $m = 1$ helicity source spheromak experiment. *Physics of Fluids B*, 1(6):1254, June 1989.

[13]Michael J. Schaffer. Exponential Taylor states in circular cylinders. *Physics of Fluids*, 30(1):160, 1987.

[14]John M. Finn, Wallace M. Manheimer, and Edward Ott. Spheromak tilting instability in cylindrical geometry. *Physics of Fluids*, 24(7):1336, 1981.

[15]G. C. Goldenbaum, J. H. Irby, Y. P. Chong, and G. W. Hart. Formation of a spheromak plasma configuration. *Physical Review Letters*, 44(6):393, 1980.

[16]T. R. Jarboe, I. Henins, H. W. Hoida, R. K Linford, J. Marshall, D. A. Platts, and A. R. Sherwood. Motion of a compact toroid inside a cylindrical flux conserver. *Physical Review Letters*, 45(15):1264, 1980.

[17]Leaf Turner. Analytic solutions of $\nabla \times B = \lambda B$ having separatrices for geometries with one ignorable coordinate. *Physics of Fluids*, 27(7):1677, 1984.

[18]K. F. Schoenberg, R. F. Gribble, and J. A. Phillips. Zero–dimensional simulations of reversed–field pinch experiments. *Nuclear Fusion*, 22(11):1433–1441, 1982.

[19]Torkil H. Jensen and Ming S. Chu. Current drive and helicity injection. *Physics of Fluids*, 27(12):2881, 1984.

[20]T. R. Jarboe and B. Alper. A model for the loop voltage of reversed field pinches. *Physics of Fluids*, 30(4):1177, 1987.

[21]R. M. Mayo, J. C. Fernández, I. Henins, G. J. Marklin, and F. J. Wysocki. Improved understanding of current drive and confinement in spheromaks. In *Conference on Controlled Fusion and Plasma Heating*, Amsterdam, 1990. European Physical Society.

[22]J. C. Fernández, Cris W. Barnes, T. R. Jarboe, I. Henins, H. W. Hoida, P. Klingner, S. O. Knox, G. J. Marklin, and B. L. Wright. Energy confinement studies in spheromaks with mesh flux conservers. *Nuclear Fusion*, 28(9):1555, 1988.

[23]W. C. Turner, E. H. A. Granneman, C. W. Hartman, D. S. Prono, J. Taska, and A. C. Smith, Jr. Production of field-reversed plasma with a magnetized coaxial plasma gun. *Journal of Applied Physics*, 52(1):175, 1981.

[24]T. R. Jarboe, I. Henins, H. W. Hoida, R. K. Linford, J. Marshall, D. A. Platts, and A. R. Sherwood. Production of field-reversed configurations with a magnetized coaxial plasma gun. In *Proceedings of the International Symposium on Physics in Open Ended Fusion Systems, Univ. of Tsukuba*, Tsukuba, Japan, April 15-18 1980.

[25]W. T. Armstrong, D. C. Barnes, R. R. Bartsch, R. J. Commisso, C. A. Ekdahl, I. Henins, D. W. Hewitt, H. W. Hoida, T. R. Jarboe, C. J. Lilliequist, R. K. Linford, J. Marshall, K. F. McKenna, J. P. Mondt, D. A. Platts, C. E. Seyler, A. R. Sherwood, E. G. Sherwood, R. E. Siemon, and M. G. Tuszewski. Compact toroid experiments and theory. In *Plasma Physics and Controlled Nuclear Fusion Research, 1980*, volume I, page 481. IAEA, Vienna, 1981. Brussels Conference.

[26]M. Yamada, H. P. Furth, W. Hsu, A. Janos, S. Jardin, M. Okabayashi, J. Sinnis, T. H. Stix, and K. Yamazaki. Quasistatic formation of the spheromak plasma configuration. *Physical Review Letters*, 46(3):188, 1981.

[27]K. Kawai, Z. A. Pietrzyk, and H. T. Hunter. Generation of poloidally rotating spheromaks by the conical theta pinch. *Physics of Fluids*, 30(8):2561, 1987.

[28]T. R. Jarboe, C. W. Barnes, D. A. Platts, and B. L. Wright. A kinked Z-pinch as the helicity source for spheromak generation and sustainment. *Comments in Plasma Physics and Controlled Fusion*, 9(4):161, 1985.

[29]T. R. Jarboe, I. Henins, A. R. Sherwood, Cris W. Barnes, and H. W. Hoida. Slow formation and sustainment of spheromaks by a coaxial magnetized plasma source. *Physical Review Letters*, 51(1):39, 1983.

[30]H. Alfvén, L. Lindberg, and P. Mitlid. Experiments with plasma rings. *Journal of Nuclear Energy, Part C: Plasma Physics*, 1:116, 1960.

[31]L. Lindberg and C. Jacobsen. On the amplification of the poloidal magnetic flux in a plasma. *Astrophysics Journal*, 133:1043, 1961.

[32]Daniel R. Wells. Observation of plasma vortex rings. *Physics of Fluids*, 5(8):1016, 1962.

[33]B. L. Wright, C. W. Barnes, J. C. Fernandez, I. Henins, H. W. Hoida, T. R. Jarboe, S. O. Knox, G. J. Marklin, R. M. Mayo, and D. A. Platts. Helicity conservation and energy confinement in CTX spheromaks. In *Plasma Physics and Controlled Nuclear Fusion Research, 1986*, volume II, page 519. IAEA, Vienna, 1987. Kyoto Conference.

[34]M. R. Brown and P. M. Bellan. Current drive by spheromak injection into a tokamak. *Physical Review Letters*, 64(18):2144, 1990.

[35]Thomas R. Jarboe. Formation and steady-state sustainment of tokamak by coaxial helicity injection. *Fusion Technology*, 15:7, Jan. 1989.

[36]R. L. Hagenson and R. A. Krakowski. Steady-state spheromak reactor studies. *Fusion Technology*, 8:1606, 1985.

[37]Cris W. Barnes, T. R. Jarboe, G. J. Marklin, S. O. Knox, and I. Henins. The impedance and energy efficiency of a coaxial magnetized plasma source used for spheromak formation and sustainment. Technical Report LA-UR-89-909, Los Alamos National Laboratory, 1989. Accepted for publication in Phys. Fluids B, 1990.

[38]Torkil H. Jensen and Ming Sheng Chu. The bumpy Z-pinch. *Journal of Plasma Physics*, 25(3):459, 1981.

[39]M. Katsurai, N. Amemiya, and A. Hayakawa. Experimental and theoretical studies on the magnetic configuration of bumpy-z-pinch/flux-core-spheromak. In *Proceedings of the 11th US-Japan Workshop on Compact Toroids*, page 138, Los Alamos, New Mexico 87545, USA, 1989 Los Alamos National Laboratory, #LA-11808-C. Held on November 8-9, 1989, Los Alamos National Laboratory, Los Alamos, NM.

[40]M. Yamada. S-1 spheromak. *Nuclear Fusion*, 25(9):1327, 1985.

[41]A. Janos, G. W. Hart, C. H. Nam, and M. Yamada. Global magnetic fluctuations in spheromak plasmas and relaxation toward a minimum-energy state. *Physics of Fluids*, 28(12):3667, 1985.

[42]G. W. Hart, A. Janos, D. D. Meyerhofer, and M. Yamada. Verification of the Taylor (minimum energy) state in a spheromak. *Physics of Fluids*, 29(6):1994, 1986.

[43]Alan C. Janos and Masaaki Yamada. Inductive sustainment of spheromaks. *Fusion Technology*, 9:58, 1986.

[44]M. K. Bevir, C. G. Gimblett, and G. Miller. Quasi–steady–state toroidal discharges. *Physics of Fluids*, 28(6):1826–1836, 1985.

[45]G. K. Morikawa. Double-toroidal hydromagnetic-equilibrium configurations within a perfectly conducting sphere. *Physics of Fluids*, 12(8):1648, 1969.

[46]M. N. Rosenbluth and M. N. Bussac. MHD stability of spheromak. *Nuclear Fusion*, 19(4):489, 1979.

[47]A. Bondeson, G. Marklin, Z. G. An, H. H. Chen, Y. C. Lee, and C. S. Liu. Tilting instability of a cylindrical spheromak. *Physics of Fluids*, 24(9):1682, 1981.

[48]Kenji Watanabe, Kazunori Ikegami, Atsuhiko Ozaki, Norio Satomi, and Tadao Uyama. Compact toroidal plasma with toroidal and poloidal magnetic fields. *Journal of the Physical Society of Japan*, 50(6):1823, 1981.

[49]K. Katayama and M. Katsurai. Three-dimensional numerical simulation of the relaxation process in spheromak plasmas. *Physics of Fluids*, 29:1939, 1986.

[50]A.G. Sgro, A.A. Mirin, and G. Marklin. The evolution of a decaying spheromak. *Physics of Fluids*, 30(10):3219, 1987.

[51]T. R. Jarboe, Cris W. Barnes, I. Henins, H. W. Hoida, S. O. Knox, R. K. Linford, and A. R. Sherwood. The Ohmic heating of a spheromak to 100 eV. *Physics of Fluids*, 27(1):13, 1984.

[52]T. Uyama, Y. Honda, M. Nagata, M. Nishikawa, A. Ozaki, N. Satomi, and K. Watanabe. Temporal evolution of the decaying spheromak in the CTCC-I experiment. *Nuclear Fusion*, 27(5):799, 1987.

[53]N. Satomi, S. Goto, Y. Honda, Y. Kato, M. Nagata, M. Nishikawa, A. Azaki, T. Takaishi, T. Uyama, and K. Watanabe. Confinement experiments and simulation on the CTCC-I spheromak. In *Plasma Physics and Controlled Nuclear Fusion Research, 1986*, volume II, page 529. IAEA, Vienna, 1987. Kyoto Conference.

[54]T. R. Jarboe, C. W. Barnes, I. Henins, H. W. Hoida, S. O. Knox, R. K. Linford, G. J. Marklin, D. A. Platts, A. G. Sgro, A. R. Sherwood, B. L. Wright, A. A. Mirin, and D. E. Shumaker. Spheromak studies on CTX. In *Plasma Physics and Controlled Nuclear Fusion Research, 1984*, volume 2, page 501. IAEA, Vienna, 1985. London Conference.

[55]J. C. Fernández, T. R. Jarboe, S. O. Knox, I. Henins, and G. J. Marklin. Ion heating and current drive from relaxation in decaying spheromaks in mesh flux conservers. *Nuclear Fusion*, 30(1):67, 1990.

[56]Tetsuya Sato and Takaya Hayashi. Three-dimensional simulation of spheromak creation and tilting disruption. *Physical Review Letters*, 50(1):38, 1983.

[57]Takaya Hayashi and Tetsuya Sato. Spheromak global instabilities and stabilization by nearby conductors. *Physics of Fluids*, 28(12):3654, 1985.

[58]Zoran Mikić and Edward C. Morse. Linear stability analysis of compact toroidal plasmas using particle simulation. *Physics of Fluids*, 30(9):2806, 1987.

[59]S. C. Jardin, M. S. Chance, R. L. Dewar, R. C. Grimm, and D. A. Monticello. Tilting and shifting modes in a spheromak. *Nuclear Fusion*, 21(9):1203, 1981.

[60]S. Jardin and U. Christensen. Stabilizing windings for the tilting and shifting modes in an inductively formed spheromak. *Nuclear Fusion*, 21:1665, 1981.

[61]F. J. Wysocki. Experimental investigation of line tying effects on the spheromak tilt mode. *Physics of Fluids*, 30(2):482, 1987.

[62]John M. Finn and Allan Reiman. Tilt and shift mode stability in spheromaks with line tying. *Physics of Fluids*, 25(1):116, 1982.

[63]M. Yamada, R. Ellis, Jr., H. P. Furth, R. Hulse, A. Janos, S. C. Jardin, D. McNeill, C. Munson, M. Okabayashi, S. Paul, D. Post, J. Sinnis, C. Skinner, Y. C. Sun, F. Wysocki, C. Chin-Fatt, A. W. DeSilva, G. C. Goldenbaum, G. W. Hart, R. Hess, R. S. Shaw, C. W. Barnes, I. Henins, H. W. Hoida, T. R. Jarboe, S. O. Knox, R. K. Linford, J. Lipson, J. Marshall, D. A. Platts, A. R. Sherwood, and B. L. Wright. Experimental investigation of the spheromak configuration. In *Plasma Physics and Controlled Nuclear Fusion Research, 1982*, volume 2, page 265. IAEA, Vienna, 1983. Baltimore Conference.

[64]H. Bruhns, C. Chin-Fatt, Y. P. Chong, A. W. DeSilva, G. C. Goldenbaum, H. R. Griem, G. W. Hart, R. A. Hess, J. H. Irby, and R. S. Shaw. Experimental studies of spheromak formation. *Physics of Fluids*, 26(6):1616, 1983.

[65]C. Munson, A. Janos, F. Wysocki, and M. Yamada. Experimental control of the spheromak tilting instability. *Physics of Fluids*, 28(5):1525, 1985.

[66]R. Hess, C. Chinfatt, C. Cote, A. DeSilva, A. Filuk, G. Goldenbaum, J. Gavreau, and F. Hwang. Structure of Maryland spheromak plasmas. In *Proceedings of the 11th US-Japan Workshop on Compact Toroids*, page 164, Los Alamos, New Mexico 87545, USA, 1989. Los Alamos National Laboratory, #LA-11808-C. Held on November 8-9, 1989, Los Alamos National Laboratory, Los Alamos, NM.

[67]R. M. Mayo, C. K. Choi, F. M. Levinton, A. C. Janos, and M. Yamada. Effect of neutral particles on the energy confinement of spheromaks. *Physics of Fluids B*, 2(1):115, 1990.

[68]James H. Hammer, Charles W. Hartman, James L. Eddleman, and Harry S. McLean. Experimental demonstration of acceleration and focusing of magnetically confined plasma rings. *Physical Review Letters*, 61(25):2843, 1988.

[69]L. J. Perkins, S. K. Ho, and J. H. Hammer. Deep penetration fuelling of reactor-grade tokamak plasmas with accelerated compact toroids. *Nuclear Fusion*, 28(8):1365, 1988.

[70]S. C. Jardin. Ideal magnetohydrodynamic stability of the spheromak configuration. *Nuclear Fusion*, 22(5):629, 1982.

[71]W. Park and S. C. Jardin. Nonlinear saturation of nonresonant internal instabilities in a straight spheromak. *Physics of Fluids*, 26(7):1871, 1983.

[72]Y. Ono, Jr. R. A. Ellis, A. C. Janos, F. M. Levinton, R. M. Mayo, R. W. Motley, Y. Ueda, and M. Yamada. Relaxation phenomena in the high-temperature S-1 spheromak. *Physical Review Letters*, 61(25):2847, 1988.

[73]F. J. Wysocki, J. C. Fernández, I. Henins, T. R. Jarboe, G. J. Marklin, and R. M. Mayo. Progress with small, high-magnetic-field spheromaks in CTX. In *Proceedings of the 11th US-Japan Workshop on Compact Toroids*, page 185, Los Alamos, New Mexico 87545, USA, 1989. Los Alamos National Laboratory, #LA-11808-C. Held on November 8-9, 1989, Los Alamos National Laboratory, Los Alamos, NM.

[74]M. Okabayashi and A. M. M. Todd. A numerical study of MHD equilibrium and stability of the spheromak. *Nuclear Fusion*, 20(5):571, 1980.

[75]P. Gautier, R. Gruber, and F. Troyon. Numerical study of the ideal-MHD stability limits in oblate spheromaks. *Nuclear Fusion*, 21(11):1399, 1981.

[76]R. M. Mayo and G. J. Marklin. Numerical calculation of Mercier beta limits in spheromaks. *Physics of Fluids*, 31(6):1812, 1988.

[77]G. J. Marklin. MHD stable high beta spheromak equilibrium. In *Proceedings of the 11th US-Japan Workshop on Compact Toroids*, page 181, Los Alamos, New Mexico 87545, USA, 1989. Los Alamos National Laboratory, #LA-11808-C. Held on November 8-9, 1989, Los Alamos National Laboratory, Los Alamos, NM.

[78]G. W. Hart, C. Chin-Fatt, A. W. DeSilva, G. C. Goldenbaum, R. Hess, and R. S. Shaw. Finite-pressure-gradient influences on ideal spheromak equilibrium. *Physical Review Letters*, 51(17):1558, 1983.

[79]Cris W. Barnes, T. R. Jarboe, I. Henins, A. R. Sherwood, S. O. Knox, R. Gribble, H. W. Hoida, P. L. Klingner, C. G. Lilliequist, R. K. Linford, D. A. Platts, R. L. Spencer, and M. Tuszewski. Spheromak formation and operation with background filling gas and a solid flux conserver in CTX. *Nuclear Fusion*, 24(3):267, 1984.

[80]Cris W. Barnes, T. R. Jarboe, H. W. Hoida, B. L. Wright, Russell A. Hulse, and D. E. Post. Zero-dimensional energy balance modeling of the CTX spheromak experiment. *Nuclear Fusion*, 25(11):1657, 1985.

[81]S. Sinman and A. Sinman. Comparative analysis at SK/CG-1 machine for spheromak plasma heating. In *Conference on Controlled Fusion and Plasma Physics*, page 807, Venice, 1989. European Physical Society. Volume 13B, Part II (Venice Conference).

[82]M. Nishikawa, Y. Kato, N. Satomi, and K. Watanabe. Pressure effect on equilibrium configuration of CTCC-II spheromak. In *Proceedings of the 11th US-Japan Workshop on Compact Toroids*, page 156, Los Alamos, New Mexico 87545, USA, 1989. Los Alamos National Laboratory, #LA-11808-C. Held on November 8-9, 1989, Los Alamos National Laboratory, Los Alamos, NM.

[83]F. J. Wysocki, J. C. Fernández, T. R. Jarboe, and G. J. Marklin. Evidence for a pressure-driven instability in the CTX spheromak. *Physical Review Letters*, 61(21):2457, 1988.

[84]A. Von Engel. *Ionized Gases*. Oxford University Press, Oxford, 1955.

[85]F. J. Wysocki, J. C. Fernandez, I. Henins, T. R. Jarboe, and G. J. Marklin. Improved energy confinement in spheromaks with reduced field errors. Technical Report LA-UR-90-767, Los Alamos National Laboratory, 1990. Submitted to Physical Review Letters.

[86]H. Y. W. Tsui. Magnetic helicity transport and the reversed field pinch. *Nuclear Fusion*, 28(9):1543, 1988.

[87]R. A. Nebel and E. J. Caramana. The role of $m = 0$ modal components in the reversed-field-pinch dynamo effect in the single fluid magnetohydrodynamics model. *Physics of Fluids B*, 1(8):1671, 1989.

[88]J. C. Fernández, R. M. Mayo, F. J. Wysocki, I. Henins, T. R. Jarboe, and G. J. Marklin. Bolometry, spectroscopy and doppler T_i measurements in high current density CTX spheromaks. In *Proceedings of the 11th US-Japan Workshop on Compact Toroids*, page 176, Los Alamos, New Mexico 87545, USA, 1989. Los Alamos National Laboratory, #LA-11808-C. Held on November 8-9, 1989, Los Alamos National Laboratory, Los Alamos, NM.

[89]F. M. Levinton and D. D. Meyerhofer. Measurement of the local particle diffusion coefficient in a magnetized plasma. *Review of Scientific Instruments*, 58(8):1393, 1987.

[90]D. D. Meyerhofer, F. M. Levinton, and M. Yamada. Particle diffusion in a spheromak. *Physical Review Letters*, 60(10):933, 1988.

[91]R. M. Mayo, F. M. Levinton, D. D. Meyerhofer, T. K. Chu, S. F. Paul, and M. Yamada. Measurement of the local carbon diffusion coefficient in the S-1 spheromak. *Nuclear Fusion*, 29(9):1493, 1989.

[92]B. Alper, H. A. B. Bodin, C. A. Bunting, P. G Carolan, J. Cunnane, D. E. Evans, A. R. Field, R. J. Hayden, A. Lazaros, A. A. Newton, P. G. Noonan, A. Patel, H. Y. W. Tsui, and P. D. Wilcock. Improved confinement in HBTX with removal of tile limiters. *Plasma Physics and Controlled Nuclear Fusion*, 30(7):843–851, 1988.

[93]M. Nagata, K. Araki, H. Furuya, H. Tatezumi, and T. Uyama. Fact spheromak experiment. In *Proceedings of the 10th US-Japan Workshop on Compact Toroids*, page 9, College of Science and Technology, 1-8 Kanda Suragadai, Chiyoda-ku, Tokyo, Japan, 1988. Nihon University. Held on November 14-16, 1988, Gohra, Hakone, Japan.

[94]P. K. Browning, B. Browning, J. Cleg, G. Cunningham, P. Dooling, S. Gee, K. Gibson, D. Kitson, M. G. Rusbridge, and K. Sebti. Progress on sphex, the spheromak at manchester. In *Proceedings of the 11th US-Japan Workshop on Compact Toroids*, page 152, Los Alamos, New Mexico 87545, USA, 1989. Los Alamos National Laboratory, #LA-11808-C. Held on November 8-9, 1989, Los Alamos National Laboratory, Los Alamos, NM.

[95]C. R. Sovinec, C. J. Clouse, J. H. Degnan, D. Dietz, and K. E. Hackett. Computational simulation of compact toroidal plasma formation. In *Proceedings of the 11th US-Japan Workshop on Compact Toroids*, page 160, Los Alamos, New Mexico 87545, USA, 1989. Los Alamos National Laboratory, #LA-11808-C. Held on November 8-9, 1989, Los Alamos National Laboratory, Los Alamos, NM.

[96]J. H. Hammer, J. L. Eddleman, C. W. Hartman, H. S. McLean, A. W. Molvik, and M. Gee. X-ray production experiments on the RACE compact torus accelerator. In *Proceedings of the 11th US-Japan Workshop on Compact Toroids*, page 202, Los Alamos, New Mexico 87545, USA, 1989. Los Alamos National Laboratory, #LA-11808-C. Held on November 8-9, 1989, Los Alamos National Laboratory, Los Alamos, NM.

[97]C. W. Hartman, J. L. Eddleman, J. H. Hammer, B. G. Logan, and A. W. Molvik. Acceleration of spheromak toruses, experimental results and fusion applications. In *Proceedings of the 11th US-Japan Workshop on Compact Toroids*, page 197, Los Alamos, New Mexico 87545, USA, 1989. Los Alamos National Laboratory, #LA-11808-C. Held on November 8 9, 1989, Los Alamos National Laboratory, Los Alamos, NM.

[98]E. C. Morse, A. Kulewiec, R. Stachowski, J. S. Hardwick, and W. B. Kunkel. Berkeley compact toroid experiment: Experimental results and progress. In *Proceedings of the 11th US-Japan Workshop on Compact Toroids*, page 148, Los Alamos, New Mexico 87545, USA, 1989. Los Alamos National Laboratory, #LA-11808-C. Held on November 8-9, 1989, Los Alamos National Laboratory, Los Alamos, NM.

[99]J.-L. Gauvreau, G. C. Goldenbaum, C Chin-Fatt, A. W. DeSilva, and R. A. Hess. Observation of wavelength profiles during formation in the Maryland Spheromak. In *Proceedings of the 11th US-Japan Workshop on Compact Toroids*, page 172, Los Alamos, New Mexico 87545, USA, 1989. Los Alamos National Laboratory, #LA-11808-C. Held on November 8-9, 1989, Los Alamos National Laboratory, Los Alamos, NM.

[100]A. B. Filuk, G. C. Goldenbaum, C. Chin-Fatt, A. W. DeSilva, and R. A. Hess. Observations and modelling of electron density on the maryland spheromak. In *Proceedings of the 11th US-Japan Workshop on Compact Toroids*, page 168, Los Alamos, New Mexico 87545, USA, 1989. Los Alamos National Laboratory, #LA-11808-C. Held on November 8-9, 1989, Los Alamos National Laboratory, Los Alamos, NM.

[101]I. Henins, J. C. Fernández, T. R. Jarboe, S. P. Marsh, G. J. Marklin, R. M. Mayo, and F. J. Wysocki. Design of a spheromak compressor driven by high explosives. In *Proceedings of the 11th US-Japan Workshop on Compact Toroids*, page 193, Los Alamos, New Mexico 87545, USA, 1989. Los Alamos National Laboratory, #LA-11808-C. Held on November 8-9, 1989, Los Alamos National Laboratory, Los Alamos, NM.

[102]D. C. Barnes. Mechanical injection of magnetic helicity. *Physics of Fluids*, 31(8):2214, 1988.

[103]R. M. Mayo, D. C. Barnes, B. Freeman, I. Henins, T. R. Jarboe, and D. Platts. Recent progress on the Hess experiment. In *Proceedings of the 11th US-Japan Workshop on Compact Toroids*, page 189, Los Alamos, New Mexico 87545, USA, 1989. Los Alamos National Laboratory, #LA-11808-C. Held on November 8-9, 1989, Los Alamos National Laboratory, Los Alamos, NM.

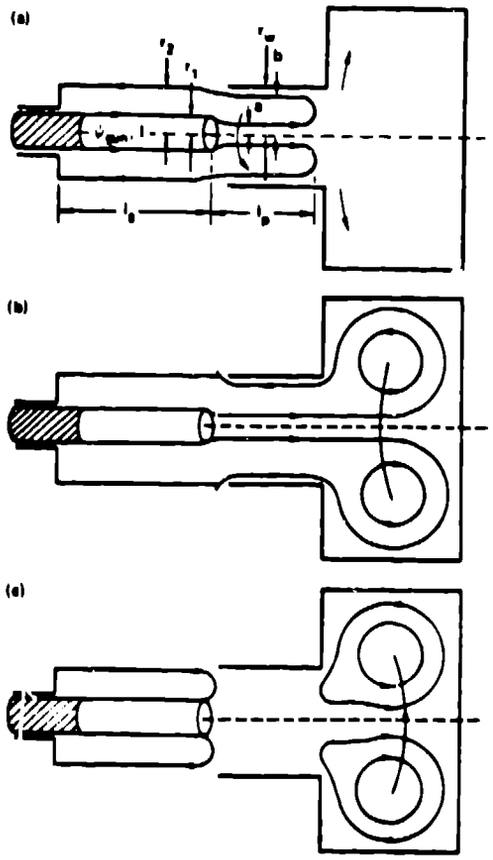

Figure 1: Spheromak formation by coaxial plasma gun.[2]

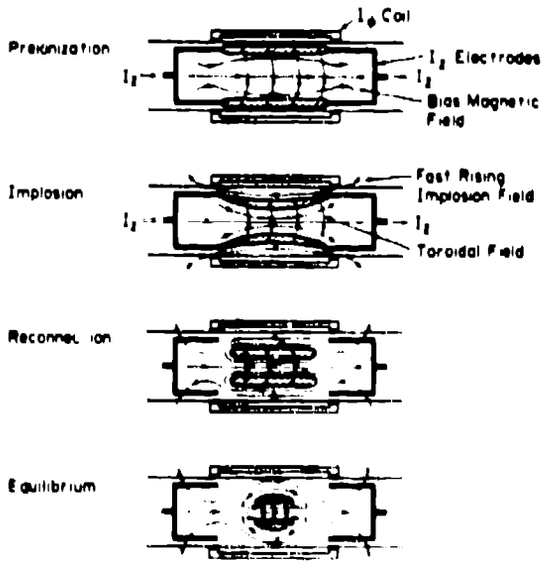

Figure 2: Spheromak formation by combined θ and z pinches.[15]

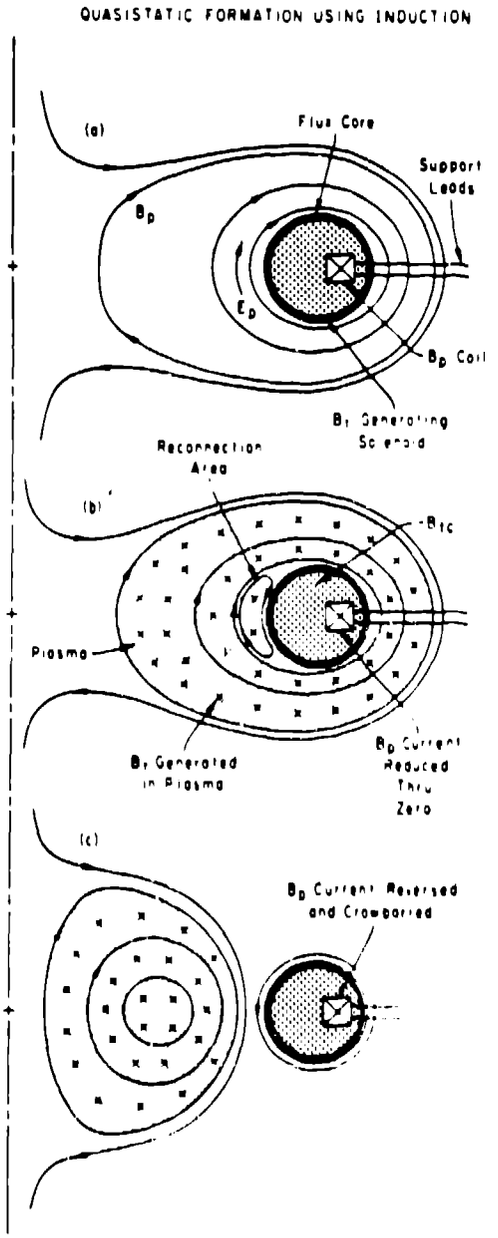

Figure 3: Spheromak formation by the flux-core method.[20]

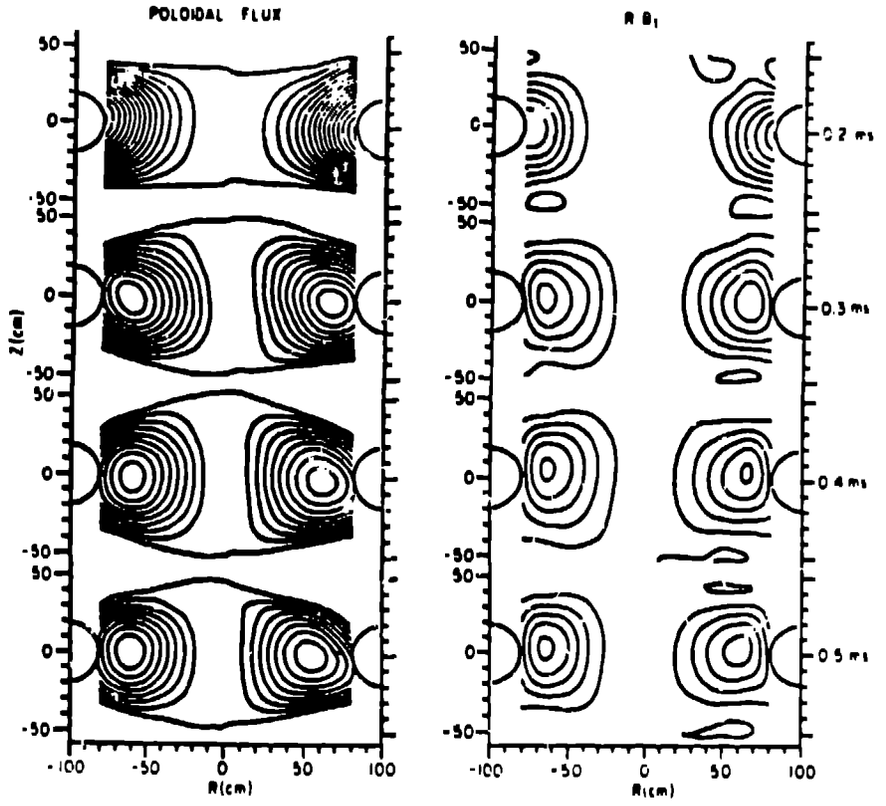

Figure 4: Poloidal and toroidal flux plots during S-1 spheromak formation obtained by internal magnetic probe data.[41,40]

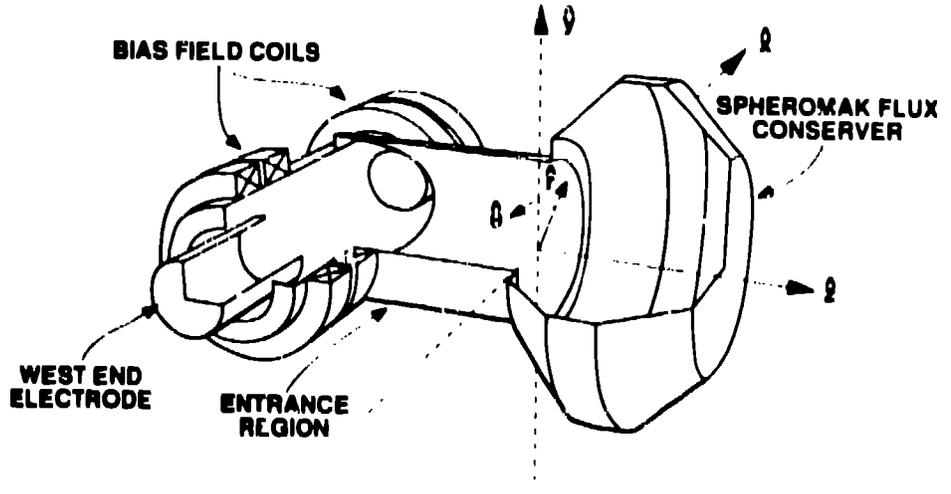

Figure 5: The $m = 1$ helicity source, entrance region, and spheromak flux conserver.[12]

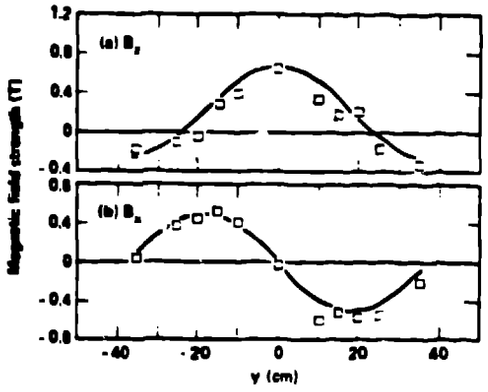

Figure 6: The measured poloidal and toroidal magnetic fields profiles in the Beta II spheromak compared to the profiles corresponding to the minimum-energy state.[2]

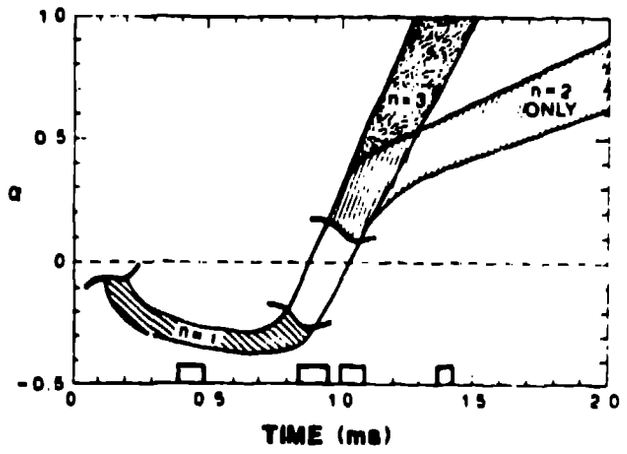

Figure 7: The measured evolution of the $\lambda(\psi)$ slope a for a typical CTX MFC discharge.[4] The shadowed regions indicate when the $\lambda(\psi)$ profiles deviate enough from the minimum-energy state ($a = 0$) so that internal kink modes are observed, in good agreement with single-fluid MHD stability theory. The helicity source was turned off at 0.7 ms in these discharges.

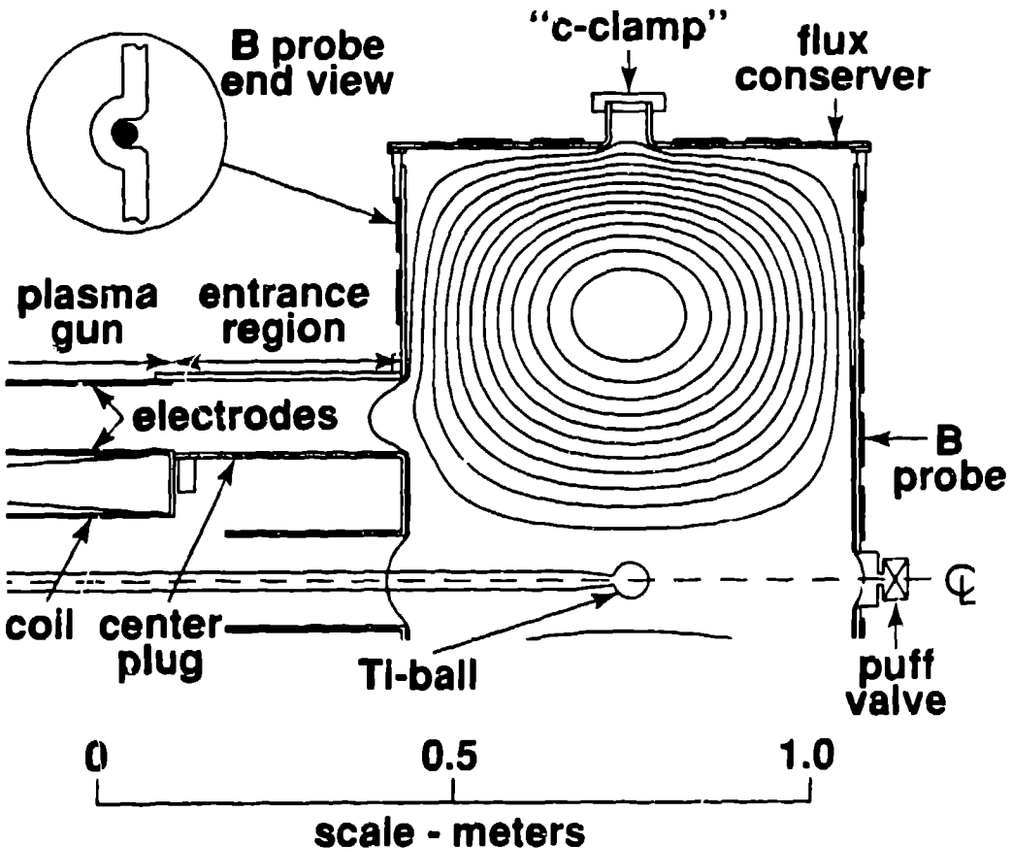

Figure 10: Geometry of the Solid Flux Conserver, entrance region and source in CTX. The poloidal flux surfaces, as calculated from the surface magnetic probe data fitted to the MHD equilibrium code results, are also shown. This flux conserver is specifically designed to minimize field errors (magnetic field penetration into the wall).[85]

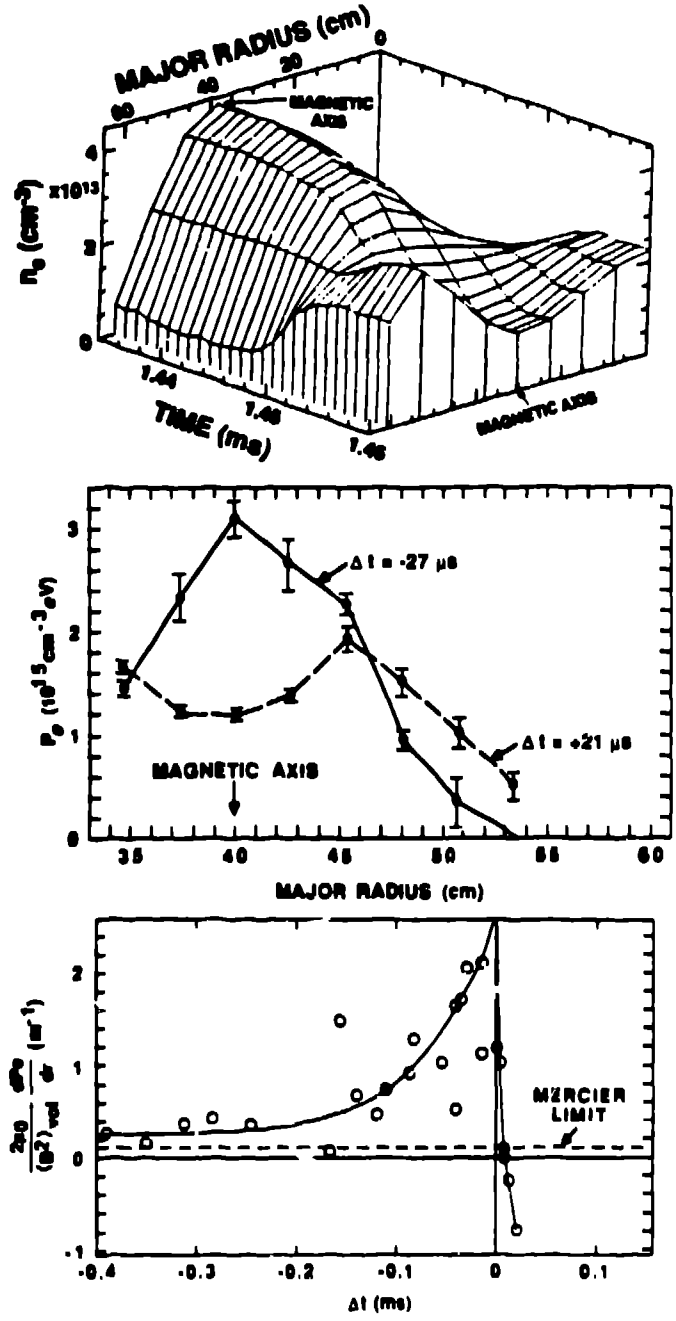

Figure 11: Pressure-driven instability in the CTX SFC. Top: Evidence for the interchange in the electron density profile, as reconstructed by from the eight-chord interferometer data; Middle: Evidence for the interchange on the electron pressure profile, as measured by the absolutely calibrated Thomson scattering diagnostic; and Bottom: Normalized electron pressure gradient increase versus time previous to the instability.[81]

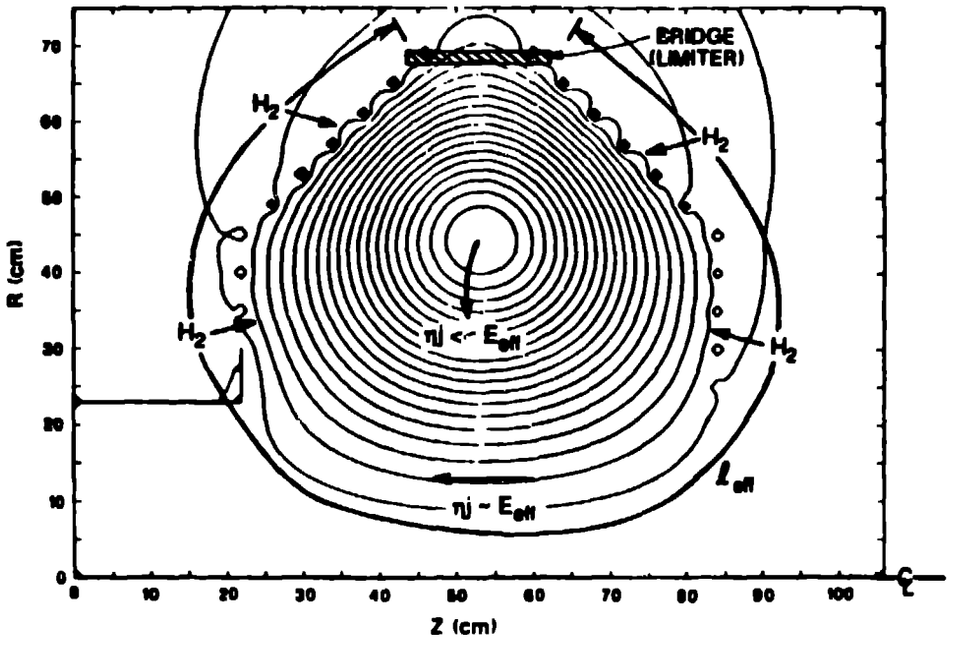

Figure 12: One-half of the CTX mesh flux conserver (MFC) cross section. Typical normalized spheromak poloidal flux contours (5% increments) during decay are included. The figure shows the typical 25% poloidal-flux fraction which intersects the wall during decay. In the figure, the poloidal field wraps around the magnetic axis in the counter-clockwise direction, while the toroidal field goes into the page. This corresponds to negative helicity ($\vec{J}$ antiparallel to $\vec{B}$).[55]

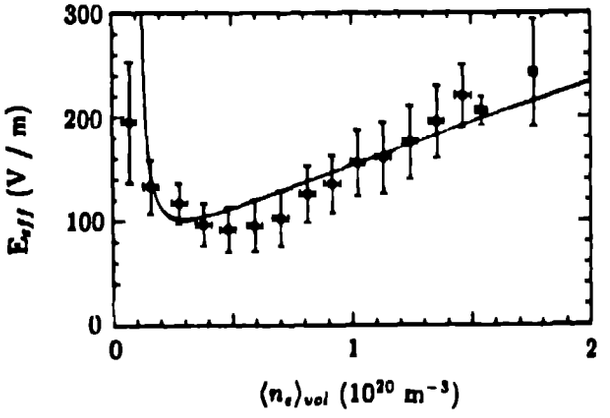

Figure 13: E_{eff} ($\approx \eta J_{\|}$ at the edge) versus electron density for the CTX MFC. The 1825 data points are averaged in 20 intervals in density, with vertical error bars representing the standard deviation of the sample in each interval. The solid curve is the equivalent Paschen curve for breakdown in hydrogen corresponding to a 10 to 1 ratio of neutral to electron density (as observed experimentally in steady state), and a field-line length of l_{eff} =3 m (approximately the length of a field line at the edge).[22]

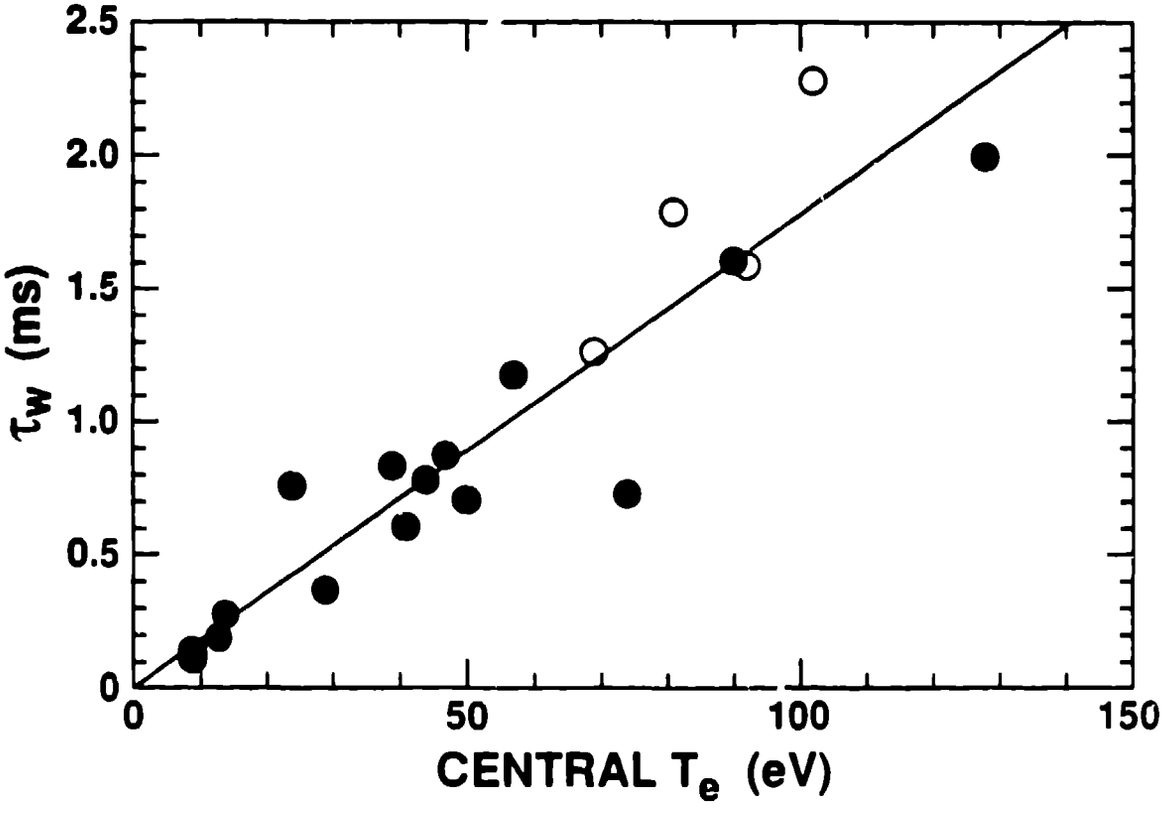

Figure 14: Plot of the magnetic energy decay time $\tau_W \equiv \tau_{H^2}$ versus central electron temperature in CTX spheromaks in the SFC. By using the electron temperature profile as determined from multi-point Thomson scattering, it has been determined that the decay rates in these discharges are consistent with the volume-averaged Spitzer resistivity with a $Z_{eff} \approx 2 \pm 1$.[85]

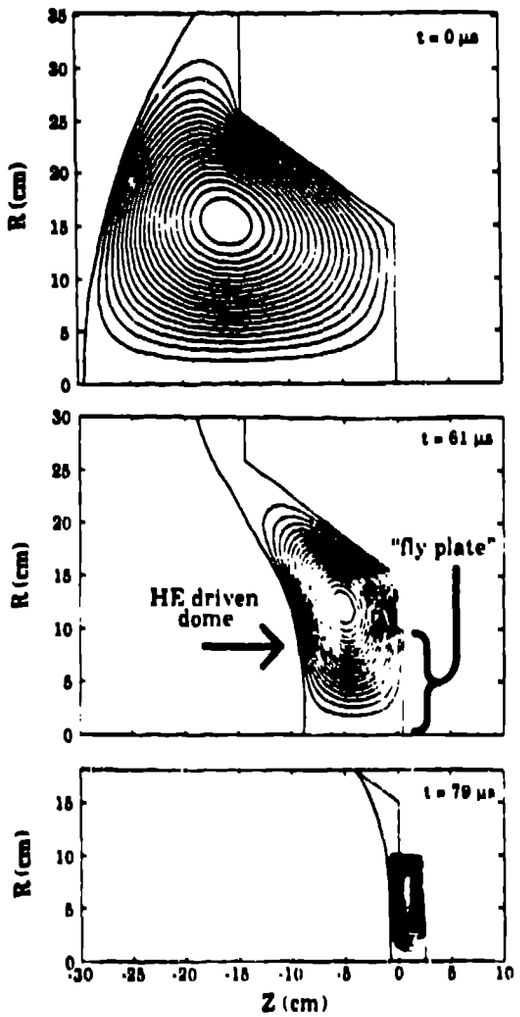

Figure 15: Numerical simulation of the spheromak dynamics (including resistive decay) under compression by a conducting dome.[7.4]

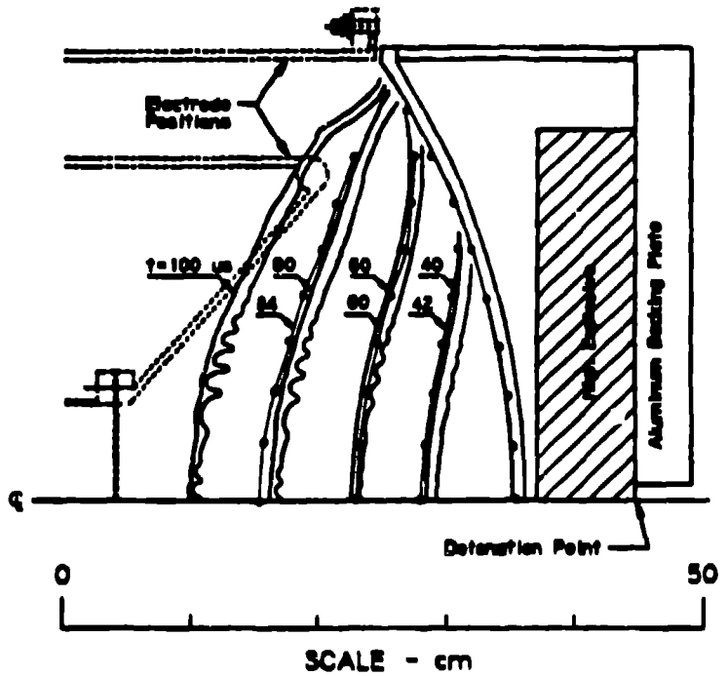

Figure 16: Comparison of the measured (dotted line) and simulated (solid lines) dynamics of an HE-driven 0.95 cm thick aluminum at various times after HE detonation at $t = 0$.[101] The dashed lines outline the entrance region and the opposite wall of the flux conserver, if they were present, as in the preceding Fig.

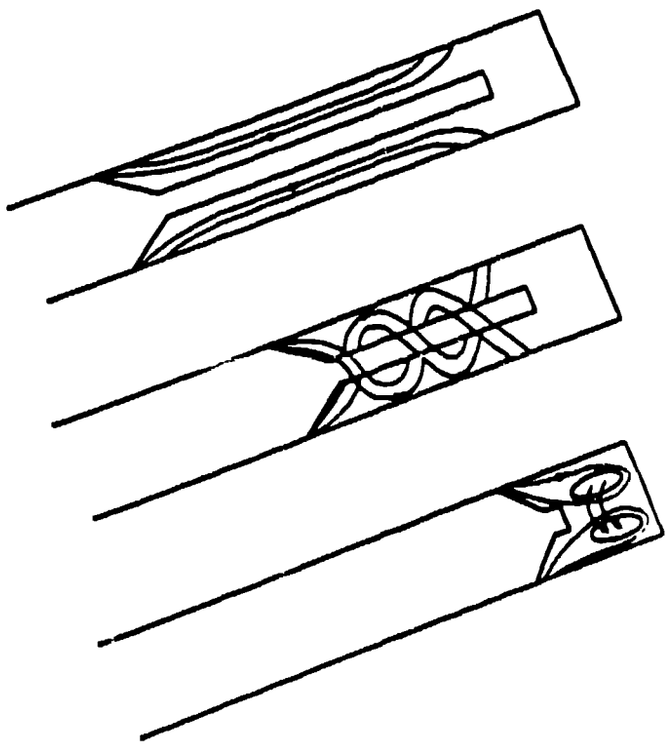

Figure 17: Mechanical helicity injection sequence.[101]